UNIVERSIDADE ESTADUAL DE CAMPINAS
INSTITUTO DE BIOLOGIA

REBEKA CATALDO DE OLIVEIRA FANTI

INVESTIGATING SMALL MOLECULE ENTRY RULES IN GRAM-NEGATIVE BACTERIA

INVESTIGANDO A ENTRADA DE PEQUENAS MOLÉCULAS EM BACTÉRIAS GRAM-NEGATIVA

CAMPINAS
2021

REBEKA CATALDO DE OLIVEIRA FANTI

INVESTIGATING SMALL MOLECULE ENTRY RULES IN GRAM-NEGATIVE BACTERIA

INVESTIGANDO A ENTRADA DE PEQUENAS MOLÉCULAS EM BACTÉRIAS GRAM-NEGATIVA

Dissertation presented to the Institute of Biology of the University of Campinas in partial fulfillment of the requirements for the degree of Master in Genetics and Molecular Biology, in the field of Microbiology.

Dissertação apresentada ao Instituto de Biologia da Universidade Estadual de Campinas como parte dos requisitos exigidos para a obtenção do Título de Mestra em Genética e Biologia Molecular, na área de Microbiologia.

Orientador: Dr. Rafael Lemos Miguez Couñago

ESTE ARQUIVO DIGITAL CORRESPONDE À VERSÃO FINAL DA DISSERTAÇÃO DEFENDIDA PELA ALUNA REBEKA CATALDO DE OLIVEIRA FANTI E ORIENTADA PELO DR. RAFAEL LEMOS MIGUEZ COUÑAGO.

CAMPINAS

2021

Ficha catalográfica
Universidade Estadual de Campinas
Biblioteca do Instituto de Biologia
Mara Janaina de Oliveira - CRB 8/6972

F218i

Fanti, Rebeka, 1992-
Investigating small molecule entry rules in gram-negative bacteria / Rebeka Cataldo de Oliveira Fanti. – Campinas, SP : [s.n.], 2021.

Orientador: Rafael Lemos Miguez Couñago.
Dissertação (mestrado) – Universidade Estadual de Campinas, Instituto de Biologia.

1. Técnicas de transferência de energia por ressonância de bioluminescência. 2. Descoberta de drogas. 3. *Escherichia coli*. I. Couñago, Rafael Lemos Miguez. II. Universidade Estadual de Campinas. Instituto de Biologia. III. Título.

Informações para Biblioteca Digital

Título em outro idioma: Investigando a entrada de pequenas moléculas em bactérias gram-negativas
Palavras-chave em inglês:
Bioluminescence resonance energy transfer techniques
Drug discovery
Escherichia coli
Área de concentração: Microbiologia
Titulação: Mestra em Genética e Biologia Molecular
Banca examinadora:
Rafael Lemos Miguez Couñago [Orientador]
Cristina Elisa Alvarez Martinez
Aled Edwards
Data de defesa: 17-05-2021
Programa de Pós-Graduação: Genética e Biologia Molecular

Identificação e informações acadêmicas do(a) aluno(a)
- ORCID do autor: https://orcid.org/0000-0001-9995-5875
- Currículo Lattes do autor: http://lattes.cnpq.br/0055764133541549

Campinas, 17 de maio de 2021

COMISSÃO EXAMINADORA

Dr. Rafael Lemos Miguez Couñago

Profa. Dra. Cristina Elisa Alvarez Martinez

Dr. Aled Edwards

Os membros da Comissão Examinadora acima assinaram a Ata de defesa, que se encontra no processo de vida acadêmica do aluno.

A Ata da defesa com as respectivas assinaturas dos membros encontra-se no SIGA/Sistema de Fluxo de Dissertação/Tese e na Secretaria do Programa de Pós-Graduação em Genética e Biologia Molecular do Instituto de Biologia

Acknowledgements

I would like to thank my supervisor, Dr. Rafael M. Couñago, for the opportunity, patience, guidance, and mentorship throughout my journey at Unicamp. Most importantly, for always pushing me to show my true potential.

To my family for all the support during this journey. In special, my siblings, Renata and Raphael, for always being by my side and motivating me even at thousands of miles away and crazy time zones. And my father, Nelson, who has taught me, by example, to be a hard worker since a young age.

To my lab colleagues for always willing to help and sharing their knowledge with me. In special, Priscila, Caio, Carol, Gustavo and Stanley who worked directly with me and were an important part of the success of this work.

To my housemates who became my second family throughout these years.

To Dr. Marcel Behr, Jaryd Sullivan and Fiona McIntosh for welcoming me in their laboratory at McGill University and sharing with me their experience and knowledge about mycobacteria, which added great value to this work.

I would like to thank the funding agency CNPQ-Conselho Nacional de Desenvolvimento Científico e Tecnológico for the financial support. (process number 130075/2020-5).

This study was financed in part by the Coordenação de Aperfeiçoamento de Pessoal de Nível Superior - Brasil (CAPES) - Finance Code 001.

"Suddenly it was clear to me that all the beautiful complexity of life had simplicity at its core"

-Eric Lander

Resumo

A maioria das pequenas moléculas, incluindo antibióticos, não conseguem ultrapassar o envelope celular bacteriano. Essa dificuldade representa um desafio para a descoberta de novas drogas contra patógenos bacterianos. Subjacente a este problema está a nossa atual incapacidade de prever quais as propriedades físico-químicas que permitem que compostos entrem e se acumulem em células bacterianas. Em contraste, as propriedades farmacocinéticas para a entrada e o acúmulo de pequenas moléculas em células humanas são bem compreendidas. Esse conhecimento foi obtido, em grande parte, através da utilização de ensaios que permitem estudar a entrada e o acúmulo de compostos em células humanas vivas e que estão facilmente ao alcance da comunidade de pesquisa. Infelizmente, os métodos atuais para avaliar o acúmulo de pequenas moléculas em bactérias não são compatíveis com a utilização de células vivas e o equipamento e a experiência necessários não estão prontamente disponíveis na grande maioria dos laboratórios de microbiologia. Em nossos estudos, desenvolvemos um novo ensaio, baseado na transferência de energia entre um doador bioluminescente e um aceptor, chamado BRET, como um meio de avaliar o engajamento de compostos e suas características de ligação com uma proteína-alvo em células bacterianas vivas. Primeiramente, o sinal de BRET foi obtido em células de *Escherichia coli* que expressam uma proteína-alvo (Diidrofolato redutase, EcoDHFR) fusionada a uma pequena e muito brilhante luciferase, a NanoLuc (doador de BRET) e na presença de um ligante fluorescente (aceptor de BRET), que é capaz de ligar-se reversivelmente à proteína-alvo em células vivas. As características de ligação de compostos foram avaliadas por sua capacidade entrar na célula, competir e deslocar o marcador fluorescente do sítio ativo da proteína-alvo, consequentemente interrompendo a transferência de energia entre o doador e o aceptor de BRET. Resultados semelhantes foram alcançados em *Micobacterium abscessus*. Uma vez bem estabelecido, validamos o ensaio em formato de alta vazão e testamos uma biblioteca de 175 inibidores de DHFR inicialmente desenvolvidos para *M. tuberculosis* e conseguimos identificar novos ligantes para DHFR e permeáveis em células de *E. coli* e *M. abscessuss*.

Abstract

Most small molecules, including antibiotics, cannot transpose the bacterial cell envelope. This difficulty poses a challenge for the discovery of new drugs against bacterial pathogens. Underlying this problem is our current inability to predict what types of physicochemical properties small molecules should display to permeate and accumulate within bacterial cells. By contrast, the pharmacokinetic properties of compounds required to accumulate in human cells are now well understood due to the wide availability of assays that can detect compound accumulation in living human cells and that are easily within reach of the research community. Unfortunately, current methods to assess small molecule accumulation in bacteria cannot be performed using living cells and the required equipment and expertise is not readily available in the vast majority of microbiology laboratories. Here we developed a novel assay, based on Bioluminesce Resonance Energy Transfer (BRET), as a means to assess compound engagement and binding characteristics with a known target in living bacterial cells. First, BRET was achieved in live *Escherichia coli* cells expressing a target protein (Dihydrofolate reductase, EcoDHFR) fused with the small and bright NanoLuc luciferase (BRET donor) and in the presence of a cell-permeable fluorescent tracer (BRET acceptor) which is capable of reversibly interacting with the target protein. The binding characteristics of a test compound are revealed by its ability to penetrate the cell-envelope, compete and dislodge the fluorescent tracer, consequently disrupting the energy transfer between the BRET donor and BRET acceptor. Later, similar results were achieved in *Mycobacterium abscessus*. Once well established, we validated the assay in a high-throughput format and tested a library of 175 DHFR inhibitors initially developed for *M. tuberculosis* DHFR and we were able to identify novel cell penetrant ligands for *E. coli* and *M. abscessus* DHFR.

Figure index

Table Index

Table of Contents

1. Introduction

1.1- Difficulties in finding new antibiotics

The discovery and development of antibiotics revolutionized the treatment of infectious disease and laid a solid foundation for modern medicine. However, a significant threat to the achievements of the antibiotic era is our current inability to counterbalance the rapid emergence of multidrug-resistant (MDR) microorganisms by not bringing new antimicrobial drugs to market fast enough[1]. In fact, large pharmaceutical companies have pulled back on antibacterial drug discovery as a result of the low return on investments and the lower success rates when compared to other therapeutic areas[2,3]. This threat has led the World health Organization (WHO) to issue warnings of an eminent post-antibiotic era, and to publish a list of bacteria for which new antibiotics are urgently needed[4], with special attention to Gram-negative bacteria, which accounts for 75% of that list.

Antibiotics have been especially difficult to develop due to the small number of well-validated molecular targets, little knowledge on compound permeability and accumulation within bacterial cells, and most importantly, the lack of methods to investigate the correlation between *in vitro* and in cell compound potency[5,6]. Historically, phenotypic screens have achieved a higher success rate for the discovery of new antibiotics, but target deconvolution is not always straightforward, which might prevent the identification of a compound mechanism of action and hamper its optimization. On the other hand, compounds developed via target-based strategies using purified proteins often fail to display in-cell activity[7,8]. Thus, it is clear that innovative technologies are needed that can merge the two approaches and generate drug-like chemical starting points with both on-target and in-cell activity.

1.2 *Escherichia coli* as a model organism

Escherichia coli is a Gram-negative bacillus that has been used as a model organism since the beginning of the 20th century. *E. coli* was the organism of choice used in the research of many breakthrough scientific findings, for example, the discovery of the genetic material[9], the description of the biological processes of transcription, translation and DNA replication[10,11,12] and the first genetically modified organism[13]. This "biological rock star" continues to play a significant role in the development of new tools for research in a variety of fields, in addition to its great biotechnological importance as it is the most studied prokaryotic model organism [14,15,16].

E. coli has many advantages as a model organism. In addition to growing fast in inexpensive, chemically defined media (doubling time of approximately 30 minutes) without forming clumps, *E. coli* also stands out as a model organism due to the vast knowledge on its genetics, well-established biological processes and the availability of a wide range of molecular tools that can be used to manipulate its genome. For instance, the use of self-replicating extrachromosomal DNA molecules, or plasmids, has been a great tool that allow us to create new *E. coli* strains very quickly. In nature, plasmids have the purpose of transferring genes horizontally among bacteria, Archea and some lower eukaryotic organisms[17], but they can be manipulated for cloning, mutagenesis, protein fusion and overexpression, and shuttling vectors from bacteria to a diverse range of hosts, to name a few applications. Furthermore, genome editing tools based on plasmids have opened doors for the creation of knockout libraries which is a great asset in the study of gene functionality. The Keio Collection[18], for example, used a plasmid based method, known as Lambda-red, to individually knockout most of non-essential genes in *E. coli*. Without a doubt, *E. coli* has been the foundation of genetic engineering and the knowledge derived from this organism can be applied for the study of its relatives in greater depth.

E. coli is a member of the Enterobacteriaceae family; microbial species of this family are diverse, usually residing in the intestines of vertebrates and contains both, non-pathogenic and pathogenic bacteria including *Salmonella*, *Klebsiella*, *Shigella*, and *Yersinia pestis*. *E. coli* is most commonly found in the lower portion of the gastrointestinal tract of mammals, where colonization occurs just a few hours after birth and a commensal relationship with the host begins. It can also be found in the environment (water and soil). As an opportunistic pathogen[19], *E. coli* can migrate to other tissues and cause extra-intestinal infections such as urinary tract infections (UTIs), newborn meningitis, pulmonary, skin and soft tissue infections, along with intestinal pathologies like Hemolytic uremic syndrome (HUS). High morbidity is observed in consequence of these

infections as HUS may lead to kidney failure[20] and newborn meningitis can cause neurologic sequelae. The recent increase in incidence of infections caused by *E. coli* has led to major outbreaks, such as the HUS epidemic in 2011 in Europe[21] and consequently, rising antibiotic resistance of these pathogens[22]. Nonetheless, Enterobacteriaceae bacteria, including *E. coli*, places third in the list of the 12 antibiotic-resistant 'priority pathogens' created by the WHO.

1.3- Bacterial cell envelope and antibiotic resistance

Most antimicrobials act by inactivating essential enzymes and cellular functions residing within the bacterial cytoplasm; these molecules must be able to cross the bacterial cell envelope before reaching their intended target. The three-layer envelope system present in Gram-negative bacteria is composed of an outer membrane, a peptidoglycan cell wall, and a cytoplasmic or inner membrane[23]. The outermost layer of the outer membrane (OM) is made of a lipopolysaccharide (LPS) and the inner part is composed of phospholipids. The OM contains protein channels known as porins which are abundant β-barrel proteins that have 16 transmembrane β strands and exhibit a trimer conformation. The peptidoglycan cell wall is a polymer made of repeating units of disaccharide N-acetyl glucosamine-N-actyl muramic acid, which are cross-linked by pentapeptide side chains that serves as a rigid exoskeleton and determines cell shape[24]. Lastly, the inner membrane (IM) is a phospholipid bilayer where membrane proteins that function in energy production, lipid biosynthesis, and protein secretion are located.

Bacterial efflux pumps recognize toxic agents, among other chemicals, that have penetrated the cell wall or toxic products generated during bacterial metabolism, and carry them out before they become a threat to the cell. According to their composition, number of transmembrane spanning regions, energy sources and substrates, bacterial efflux pumps are classified into five distinct families[23]. One of these, the resistance-nodulation-division (RND) family, is exclusive to Gram-negative bacteria and is strongly associated with clinically significant antibiotic resistance[25].

Thus, the cell envelope of Gram-negative bacteria represents a major obstacle for the discovery of new antibiotics. To reach the cytoplasm of Gram-negative bacteria, a compound must transpose two membranes with orthogonal characteristics. Hydrophilic or charged solutes can cross the outer membrane via porins[26,27], but these molecules cannot penetrate the cell membrane unless they are actively transported. To remain in the cytoplasm, compounds must avoid a large collection

of efflux pumps (such as the acrAB-tolC multidrug efflux pump) that actively pump out xenobiotics, such as antibiotics[28,29].

1.4- Methods to study compound entry into cells

Understanding permeability of small molecules across bacterial cell envelope requires quantitative methods to assess the intracellular concentration of these compounds. To this end, multiple techniques have been developed that measure the accumulation of radiometric or fluorescent versions of the compound under investigation[30]. Both radiometric and fluorescent-based methods provide fast read-outs and require minimal manipulation to the cells. However, a major drawback of these methods is that they are limited by the availability of radiolabeled compound and fluorescent moieties; and, consequently, are not amenable to the diverse compound libraries and high-throughput methods used in a drug discovery pipeline. To address these limitations, liquid chromatography-mass spectrometry (LC-MS)-based methods have been developed that can quantify drug accumulation within bacterial cells[6]. LC-MS is an extremely sensitive technique, but requires intensive sample manipulation to isolate and lyse cells prior to analyses.[31,32]

Compounds targeting Gram-negative bacteria must transpose both outer and inner membranes and evade efflux pumps. To better understand physicochemical entry rules into these bacteria, a number of additional tool cell lines and compounds have been employed. *E. coli* strains lacking acrAB-tolC are useful to assess the impact of efflux pump on compound residence time[33]. Likewise, the effect of the outer membrane in compound permeability can be investigated using outer membrane-destabilizing compounds polymyxin-b nonapeptide (PMBN) and colistin[34,35], as well as outer membrane mutant strains. Finally, *E. coli* protoplasts (lacking both outer membrane and peptidoglycan layers) can be generated to investigate inner membrane permeability to compounds[36].

1.5- A novel energy transfer technique to study compound entry in bacteria

In recent years, resonance energy transfer (RET) methods have gained a lot of attention withing the drug discovery research as its applications have extended from measuring protein-

protein interactions[37–39], to compound permeability and target engagement as well as compound residence time[40,41]. Most importantly, RET allows these dynamic interactions to be measured in live, intact cells and under physiological conditions. Fluorescence Resonance Energy Transfer (FRET) and Bioluminescence Resonance Energy Transfer (BRET) are two common ways to achieve RET in real time. While FRET relies on two fluorescent molecules and requires the donor to be excited by an external light source in order to transfer energy to the acceptor, BRET uses a luciferase as donor which generates intrinsic luminescence by the oxidation of its substrate[42]. Both are well established methods, however BRET has shown higher assay sensitivity when compared to FRET[43] and FRET-based assays are usually associated with technical problems such as photobleaching of the donor and simultaneous excitation of the donor and acceptor as a result of the extrinsic donor excitation, as well as autofluorescence. By using a bioluminescent donor, BRET bypasses some of these problems.

The bioluminescent donor used in BRET target engagement assays is a target protein fused with a luciferase. The NanoLuc luciferase has been the luciferase of choice for these assays as it is small (19 kDa), which is important for not interfering with the activity of target protein; and produces high intensity and stable luminescence with a relatively narrow spectrum, allowing spectral separation from the fluorophore present in the acceptor[44]. Another advantage of using NanoLuc is that due to its high intensity luminescence, there is usually no need to overexpress the target-fused BRET donor. The BRET acceptor, or tracer, is a bifunctional molecule composed of a ligand of the target protein attached to a fluorophore that has excitation wavelength overlapping with the emission wavelength of the BRET donor in order to be able receive the energy provided by the donor and emit fluorescence in a different wavelength (Figure 1A).

When cells expressing the BRET donor are incubated with the tracer, it penetrates the cell envelope and reversibly binds to the target protein, allowing the fluorophore and the NanoLuc to be in close proximity (< 50 Å)[45]. NanoLuc utilizes furimazine as substrate to produce luminescence peaking at 450 nm. Once furimazine is added to the medium the luminescence is then used to excite the fluorophore present in the tracer, which in turn, emits fluorescence peaking at 590 nm. Compounds that can enter the cell and interact with the binding site of the target protein will displace the tracer from the active site of the target protein, consequently causing a reduction of the BRET signal (Figure 1 B and C). While BRET has found widespread use to study target engagement in mammalian cells, it has never been employed for this purpose in bacterial cells.

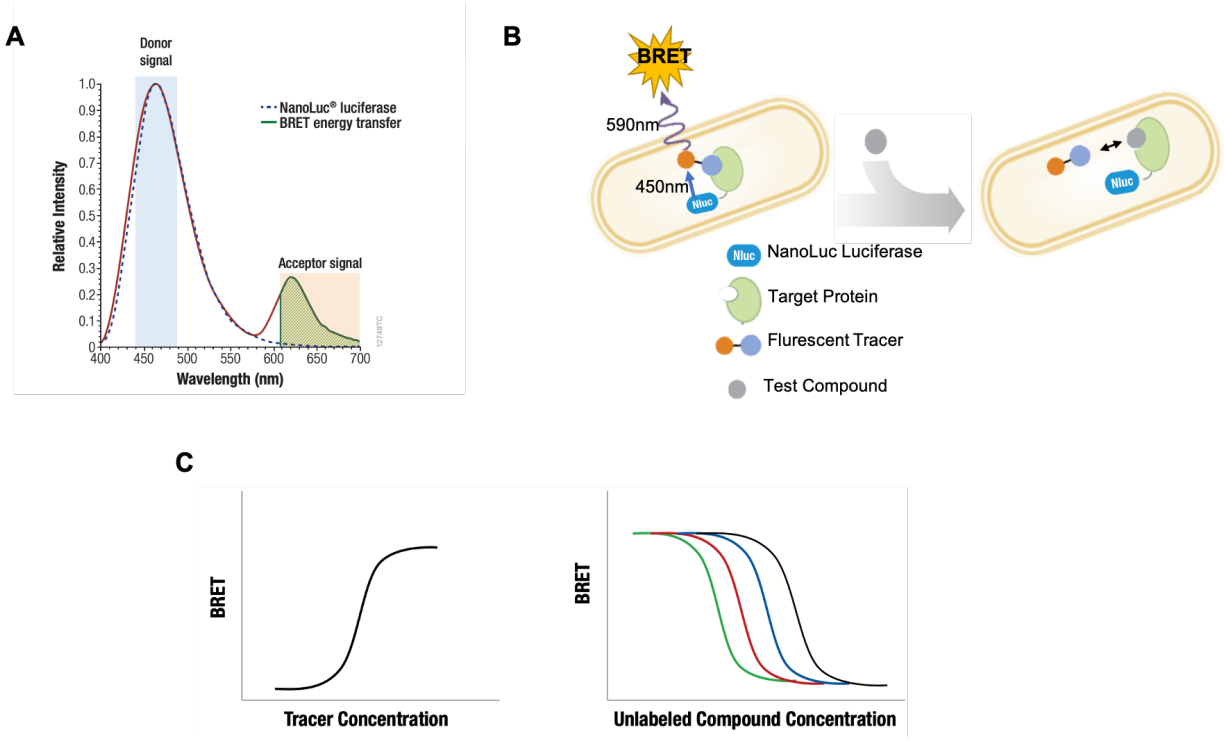

Figure 1- Overview of the NanoBRET assay.

A) Spectral separation of the luminescence emitted by the NanoLuc (450 nm) and the fluorescent tracer (590 nm). **B)** Schematic representation of the bacterial BRET. **C)** Expected BRET curves for: the titration of tracer onto BRET donor reveals the affinity between BRET donor and BRET acceptor (left panel); the titration of test compounds in the presence of a fixed concentration of tracer (right panel). Different colors indicate different compounds with different affinities with target.

2. Justification

Given the urgent need of novel tools to expedite the discovery of new antibiotics, the development of a BRET-based assay for bacteria would allow, among other things, the research community to investigate compound entry and target engagement within living bacterial cells. BRET-based assays can be used in a high-throughput format, thus allowing large compound libraries to be screened in a single experiment, and requires minimal manipulation to the cells. Moreover, BRET detection and data analysis is easily achievable using widely available equipment (a luminometer microplate reader) and user-friendly software (e.g.: graphpad).

3. Objectives

General Objective

The main goal of this work was to develop a BRET-based assay in the Gram-negative bacteria *Escherichia coli* using the essential enzyme Dihydrofolate Reductase (EcoDHFR) fused with the NanoLuc luciferase as a BRET donor, and the well-known EcoDHFR inhibitor, Trimethoprim, attached with a red-fluorescent fluorophore as the BRET acceptor. Secondly, we aimed to use the BacBRET as means of studying compound entry and accumulation in *E. coli* cells using a DHFR compound library initially designed for *M. tuberculosis* DHFR. Lastly, we intended to test this assay in other bacteria.

Specific Objectives

I. Genetic engineering and recombinant production of a BRET donor (NanoLuc-fused EcoDHFR).
II. Verify the activity of both components of the BRET donor (NanoLuc and EcoDHFR) *in vitro*.
III. Characterize the binding of Trimethoprim (TMP)-based tracers to the purified BRET donor.
IV. In cell protocol optimization.
V. Evaluate permeability of TMP-based tracers in *E. coli* cells.
VI. Validate BRET in a 384-well plate format.
VII. Demonstrate the utility of the BRET assay through displacement of the tracer.
VIII. Screen and evaluate compound entrance and accumulation of a DHFR compound library.

4. Material and Methods:

4.1 Bacterial Strains and growth conditions

For the cloning steps, chemically competent *E. coli* MACH1 was used. *E. coli* BL21(DE3)-R3-pRARE2 was used for recombinant protein production, while *E. coli* BL21(DE3) was used in BRET assays and microscopy imaging. *E. coli* BW25113, BW25113 ΔTolC and *M. abscessus* were used in BRET assays. Table 1 summarizes the bacterial strains utilized throughout this project and their characteristics.

Table 1- Description of the Bacterial strains

Species	Strain	Characteristic	Reference
Escherichia coli	MACH1	Fast growing *E. coli* derivative of W strains.	Invitrogen
	BL21(DE3)	*E. coli* B strain with DE3, a λ prophage carrying the T7 RNA polymerase gene and *lacI*^{q}.	F. William Studier & Barbara A. Moffatt, 1986
	BL21(DE3)-R3-pRARE	Derivative of BL212(DE3) containing the plasmid pRARE2 (Cm^{r}), carrying seven rare-codon tRNA genes.	Savitsky et al. 2010
	BW25113	*E. coli* K-12 strain. Parent strain for Keio Collection single-gene knockout strains.	Baba et al. 2006
	BW25113 ΔTolC	Mutant of BW25113 (WT). TolC gene knockout and replaced with a kanamycin cassette (Km^{r}).	Baba et al. 2006
Mycobacterium abscessus subsp. *abscessus*	ATCC 19977	*M. abscessus* smooth reference strain.	Gupta et al. 2018

For selecting transformants, *E. coli* was plated on LB agar (yeast extract 5 g/L; tryptone 10 g/L; NaCl 10 g/L; agar 15 g/L; pH 7.5) and grown overnight at 37 °C, while *M. abscessus* was plated on Middlebrook 7H10 (Difco laboratories) supplemented with 10% OACD (oleic acid-albumin-dextrose-catalase) and 0.5 % glycerol and incubated at 37 °C for 3 to 5 days.

Recombinant protein production used TB medium (yeast extract 24 g/L; tryptone 20 g/L; glycerol 4 mL/L; KH_2PO_4 23 g/L; K_2HPO_4 15 g/L; pH 7.2). For BRET measurements, viability assays and microscopy imaging, *E. coli* was grown in M9 Minimal Media (Na_2HPO_4 12 g/L; KH_2PO_4 3 g/L; NaCl 0.5 g/L; NH_4Cl 1 g/L; pH 7) supplemented with 0.5% glucose (w/v) and 2 mM $MgSO_4$. *M. abscessus* was grown in Middlebrook 7H9 (Difco laboratories) supplemented with 10% ACD (albumin-dextrose-catalase), 0,5% glycerol (v/v) and 0.05% Tween-80 (v/v). *E. coli* and *M. abscessus* were grown at 37 °C at 160 r.p.m. until desired the desired OD_{600} was reached.

When appropriate, media were supplemented with of ampicillin (100 µg/mL), kanamycin (50 µg/mL) or chloramphenicol (35 µg/mL). Bacterial strains were stored in -80 °C in glycerol at 12% final concentration.

4.2 Vectors, constructs and oligonucleotides

DNA vectors and constructs, and oligonucleotides used in this work are described in Tables 2, 3 and 4, respectively:

Table 2-Description of vectors used in this work.

Vector	Features	Reference
pNIC28-Bsa4	N-terminal His_6 tag, T7 promoter, TEV protease cleavage site, sites for LIC cloning, *sacB* gene allows negative selection, Km^r.	Savitsky et al. 2010
pBAD24	Arabinose inducible expression vector, P_{BAD} promoter, araC, Amp^r	Guzman et al. 1995
pMV306hsp	Mycobacteria integrating vector, P_{hsp60} promoter, Km^r.	Andreu et al. 2010

Table 3- Description of constructs utilized in this work.

Construct	Description
pNIC28_NLuc_EcoDHFR	N-terminal NanoLuc fusion with EcoDHFR transformed into BL21(De3) and BL21(De3)-R3-pRARE2 and used for protein expression and purification, BRET assays, viability assays
pNIC28_EcoDHFR_NLuc	C-terminal NanoLuc fusion with EcoDHFR transformed into BL21(De3)-R3-pRARE2 and used for protein expression and purification.
pNIC28_NLuc_EcoDHFR(M20V)	N-terminal NanoLuc fusion with mutant EcoDHFR transformed into BL21(De3)-R3-pRARE2 and used for protein expression, purification and BRET assays.
pBAD24_NLuc_EcoDHFR	N-terminal NanoLuc fusion with EcoDHFR transformed into Keio collection strains and used for BRET assays.
pMV306_NLuc_MabsDHFR	N-terminal NanoLuc fusion with MabsDHFR, transformed into *Mycobacterium abscessus* subsp. *abscessus* and used for BRET assays.

Table 4- Sequence and label of the oligonucleotides used in this work.

Primer	Sequence (5'→3')	Template DNA
NanoLuc-LIC FWD	TACTTCCAATCCATGGTCTTCACACTCGAAGATTTCGTTGG	NanoLuc-AAK1 fusion vector
NanoLuc-LIC RV	TATCCACCTTTACTGGGATCCAGCGATCGCGCCGCTC	
BamHI_EcoDHFR_HindIII FWD	CGCGGATCCATGATCAGTCTGATTGCGGCG	*E. coli* MACH1 gDNA
BamHI_EcoDHFR_HindIII RV	CCCAAGCTTTTACCGCCGCTCCAGAATC	
EcoDHFR-LIC FWD	TACTTCCAATCCATGATCAGTCTGATTGCGGTAG	*E. coli* MACH1 gDNA
EcoDHFR-LIC RV	TATCCACCTTTACTGGGATCCCCGCCGCTCCAGAATCTCAAAGCAATAG	
BamHI_NanoLuc_HindIII FWD	CGCGGATCCGTTTCTCTCGGCTCGAGCGG	BTK-NanoLuc fusion vector
BamHI_NanoLuc_HindIII RV	CCCAAGCTTTTACGCCAGAATGCGTTCGCACAG	
EcoDHFR-M20V FWD	CATGGAAAACGCCGTGCCGTGGAACCTG	pNIC28_ NLuc_EcoDHFR
EcoDHFR-M20V RV	CAGGTTCCACGGCACGGCGTTTTCCATG	
XbaI_NLuc_EcoDHFR FW	CGCTCTAGAATGCACCATCATCATCATCATTC	pNIC28_ NLuc_EcoDHFR
pLIC FWD	TGTGAGCGGATAACAATTCC	Variable-Sequencing primers
pLIC RV	AGCAGCCAACTCAGCTTCC	
pBAD24 FWD	CGGATCCTACCTGACGCTTTTTATCG	Variable-Sequencing primers
pBAD24 RV	CCAGGCAAATTCTGTTTTATCAGAC	
pMV306 FWD	CCTGATTCTGTGGATAACCGTATTACC	Variable-Sequencing primers
pMV306 RV	CGGACAAACAACAGATAAAACGAA AGG	
TolC-set2 FWD	CAGTTTGATCGCGCTAAATACTGCT	BW25113(WT) and BW25113ΔTolC
TolC-set2 RV	CTTTACGTTGCCTTACGTTCAGACG	

4.3 Construction of expression vectors

For the construction of the expression vectors, the coding sequences of NanoLuc and EcoDHFR were PCR-amplified using the High-Fidelity Phusion DNA Polymerase (NEB-USA). The oligonucleotides and templates were previously described in Table 4. PCR reactions were prepared as follows:

Reagent	**Volume (μL)**
5X Reaction buffer	10 μL
dNTP mix (10 mM each)	1.0
DMSO	1.5
Forward Primer (10 μM)	2.0
Reverse Primer (10 μM)	2.0
Phusion Polymerase	0.5
DNA Template (100 ng)	1.0
Milli-Q water	to 50 μL final volume

Template amplification followed a "touchdown" strategy having PCR cycles consisting of one initial denaturation step at 98 °C for 5 min, then 5 cycles of 98 °C for 30 secs, 68 °C for 30 secs and 72 °C for 1 min, then a total of twenty five repeats of denaturation (98 °C for 30 secs), annealing (variable temperature for 30 secs), and elongation (72 °C for 1 min) steps, followed by a final extension step at 72 °C for 5 min. Annealing temperatures were: 60 °C (cycles 1-5), 55 °C (cycles 6-10) and 52 °C (cycles 11-25). Amplicons were later analyzed by electrophoresis on a 1% agarose gel.

DNAs of interest were introduced into pNIC28-Bsa4 using a two-step cloning strategy. The first step used a Ligation Independent Cloning (LIC)[46] approach, whereas the second step utilized restriction enzymes. To produce a N-terminally-fused NanoLuc in frame with EcoDHFR, the coding sequence for NanoLuc was introduced into pNIC28_Bsa4 via LIC, resulting in the bacterial expression vector pNIC28-Bsa4_NanoLuc. This plasmid was later digested with the restriction enzymes *BamHI* and *HindIII* (Promega- USA) following the manufacturer's protocol. PCR-amplified EcoDHFR was treated with the same enzymes and then joined to the digested plasmid using T4 DNA Ligase, creating the final expression vector pNIC28-Bsa4_NanoLuc_EcoDHFR. To generate a C-terminal NanoLuc fusion, EcoDHFR was introduced into pNIC28-Bsa4 via LIC, generating the expression vector pNIC28-Bsa4_EcoDHFR. This plasmid was digested with *BamHI* and *HindIII*. NanoLuc was introduced into the digested plasmid pNIC28-Bsa4_EcoDHFR using T4 DNA Ligase, producing the expression vector pNIC28-Bsa4_EcoDHFR_NanoLuc. The resulting fusion proteins have a flexible Gly-Ser-Ser-Gly-Ala-Ile-Ala-Gly-Ser linker between NanoLuc and EcoDHFR amplified from the DNA template with the NanoLuc gene (Figure 2).

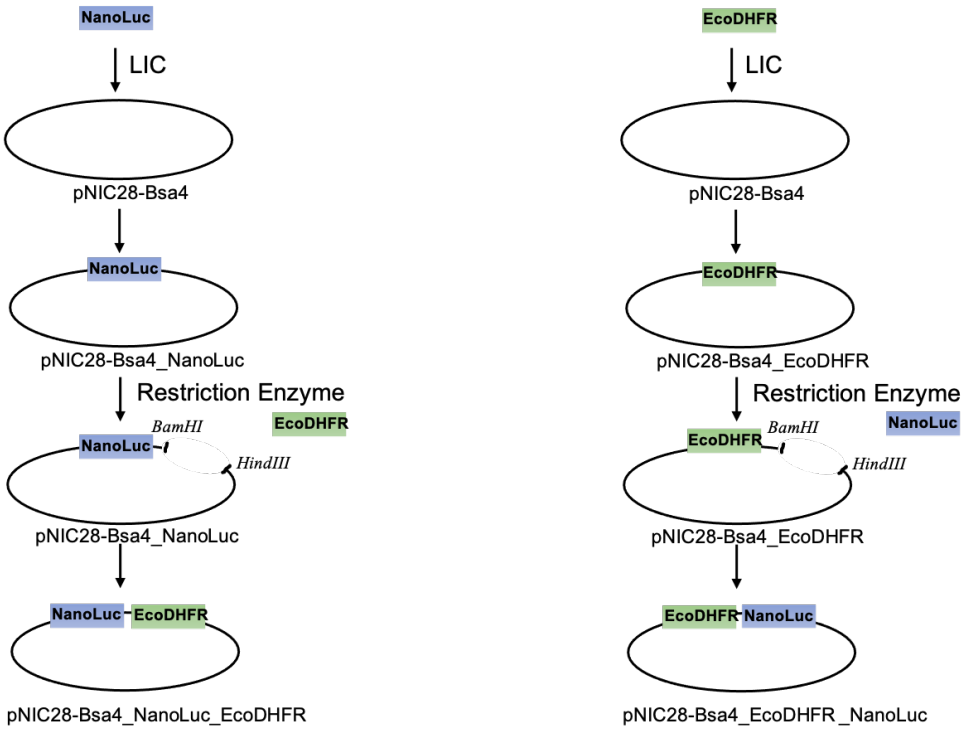

Figure 2- Overview of the cloning strategy used to create plasmids for the expression of BRET donors in E. coli. Colored boxes indicate the coding sequences for EcoDHFR (green) or NanoLuc (purple).

Once cloned into pNIC28-Bsa4, the entire NanoLuc_EcoDHFR cassette was transferred to pBAD24 and pMV306hsp using restriction enzymes. First, NanoLuc_EcoDHFR was amplified by PCR using primers containing *XbaI/HindIII* and *NotI/HindIII* restriction sites (Table 4), respectively, and pNIC28-Bsa4_NanoLuc_EcoDHFR as template. Later, the amplicons were ligated into the previously digested vector. Restriction enzymes used in this work were purchased from Promega-USA.

To generate a mutant version of the BRET donor that contains a point mutation in the EcoDHFR portion of the recombinant protein, a one-step Site-Directed Mutagenesis approach was used with primers containing the desired nucleotide substitution (ATG→GTG), the vector pNIC28-Bsa4_NanoLuc_EcoDHFR was used as template and a 5-minute extension time during the PCR cycles. All constructs were verified by DNA sequencing.

4.4 Transformation

Chemically competent BL21(De3) and BL21(De3)-R3-pRARE2 were transformed by heat shock at 42 °C for 60 seconds, then recovered in SOC medium for 1 hour at 37 °C with constant shaking and plated on LB agar plates supplemented with appropriated antibiotic for selection.

For the preparation of electrocompetent *E. coli* BW25113, BW25113 ΔTolC and *M. abscessus* cells, a 5-mL overnight culture was used to inoculate 50 mL of liquid media. The inoculum was then, grown until OD_{600} of ≈0.6. Cells were cooled on ice for 20 minutes, washed 3 times by centrifugation at 3900 r.p.m. in 10% ice-cold glycerol and lastly concentrated 100-fold.

For electroporation, 0.5- 1 µg of plasmid DNA was mixed with 100 µL of electrocompetent cells in a 0.2 cm electroporation cuvette (Bio-Rad). Electroporation was done at 2.5 kV, 25 µF and 200 Ω using the Bio-Rad Gene Pulser Xcell Electroporation System. Cells were recovered in 1 mL of liquid media, SOC for *E. coli* and 7H9 for *M. abscesus*s, for 3 hours at 37 °C and 160 r.p.m..

4.5 Small-scale protein production test

Competent *E. coli* BL21(DE3)-R3-pRARE2 were transformed with the appropriate vectors and allowed to grow on solid media overnight at 37 °C. Colonies were used to inoculate 0.5 mL of medium in a 96 deep-well block and grown overnight at 37 °C in the presence of kanamycin and chloramphenicol. 20 µL of the overnight culture was used to inoculate 1 mL of fresh TB medium containing kanamycin and allowed to grow until OD_{600} reached 2-3 (approximately 5 h) in a block shaker at 37 °C. Cultures were then allowed to cool down in an incubator at 18 °C for 30 min prior to the addition of 0.1 mM of IPTG (final concentration). The 96 deep-well block was incubated overnight at 18 °C with shaking at 900 r.p.m..

Next, the deep-well block was centrifuged at 3,500×g for 20 min at 4 °C and the medium was discarded. 200 µL of Lysis Buffer (50 mM HEPES, pH 7.5, 0.5 M NaCl, 10% glycerol, 10 mM imidazole, 0.1% DDM, 0.5 mM TCEP, 1 mM $MgCl_2$, protease inhibitors (1:200), lysozyme 0.5 mg/ml and benzonase 50 units/ml) was used to suspend the cell pellet. To lyse the cells, the deep-well block was placed at -80 °C for 20 minutes until the pellets were completely frozen and thawed in a water bath at room temperature for approximately 15 minutes. The block was then centrifuged at 3,500×g for 10 min and the supernatant transferred to a new 96 deep-well block. 50

μL of previously-equilibrated Ni^{2+}-NTA resin was added to each well and the block was placed at 4 °C for 1 h with shaking at 300 r.p.m.. The contents of each well were transferred to a 96-well filter plate, placed on a vacuum manifold and filtered. 200 μL of Wash Buffer (50 mM HEPES, pH 7.5, 0.5 M NaCl, 10% glycerol, 0.5 mM TCEP and 30 mM imidazole) was added to each well and samples were filtered again. 50 μL of Elution buffer (50 mM HEPES, pH 7.5, 0.5 M NaCl, 10% glycerol, 0.5 mM TCEP and 300 mM imidazole) was added to each sample and the filter plate was incubated in a block shaker for 10 minutes at 300 r.p.m. at 4 °C. Protein was eluted and collected by centrifugation at 300 x*g* for 3 minutes. Eluates were analyzed by electrophoresis in denaturing SDS-PAGE gels.

4.6 Protein Expression and Purification (large scale)

Colonies of *E. coli* BL21(DE3)-R3-pRARE2 containing the appropriate constructs were used to inoculate 50 mL of LB and allowed to grow overnight at 37 °C under aeration (150 r.p.m.). The starter cultures were used to inoculate 1 L of TB medium in baffled shake flasks left at 37 °C under agitation until the OD_{600} reached 1.0. Cultures were then cooled to 18 °C, 0.65 mM of IPTG was added and cells were allowed to grow for 16 h under agitation at 140 r.p.m..

Cells were harvested by centrifugation for 15 min at 7,500×g at room temperature. The cell pellet was suspended in Binding buffer (25 mM Tris-HCL, pH:8.0, 300 mM NaCl, 5% glycerol, 1 mM TCEP) and sonicated. To reduce sample viscosity due to bacterial DNA, polyethyleneimine (pH 7.5) was added to the lysate to a final concentration of 0.15% (w/v) and the sample was centrifuged at 53,000×g for 45 min at 4 °C. The supernatant was loaded onto an Immobilized Metal Affinity Chromatography (IMAC) column (2.5 ml/min, 5 mL HisTrap FF Crude), washed in binding buffer containing 30 mM imidazole and eluted in elution buffer (binding buffer with 300 mM imidazole). The eluted protein was further purified using a size-exclusion column (Superdex 200 16/60, GE Healthcare), previously equilibrated in GF buffer (20 mM HEPES pH 7.5, 300 mM NaCl, 5% glycerol, 1 mM TCEP). Fractions were analyzed by SDS-PAGE and LC-MS. The purified protein was aliquoted, flash-cooled in a liquid nitrogen bath, and stored at -80 °C until use.

4.7 BRET Measurements

For in-cell BRET assays, bacteria expressing the NLuc_EcoDHFR fusion protein were grown to log phase (OD_{600} 0.4-0.6). For *in vitro* BRET measurements, the purified BRET donor was diluted to a final concentration of 15 pM in PIPES and Tween Buffer (0.5 M PIPES, 0.2% Tween, pH: 7.3) containing excess NADPH (900 µM). Tracer was diluted in 100% DMSO to 100X the final assay concentration, then further diluted to 20X working concentration in Tracer Dilution Buffer (TDB - 12.5 mM HEPES, pH 7.5; 31.25% PEG 400). Test compounds were diluted to 1,000X final concentration in 100% DMSO, then further diluted to 10X final concentration in Assay Medium. Final concentration of DMSO in BRET assays was 1%.

85 µL of cells or purified BRET donor, 5 µL of the 20X Tracer Dilution and 10 µL of 10X diluted test compounds were dispensed in a white 96-well flat bottom, non-binding plate (Greiner-cat. 655083) and incubated for 30 min at room temperature prior the addition of the substrate and NanoLuc extracellular inhibitor cocktail at a final concentration recommended by the manufacturer (Promega-USA). Luminescence was measured in a BMG LABTECH Clariostar luminometer, using the monochromator at 460-10 nm for BRET donor and a LP 610-20 nm filter for BRET acceptor, 0.5 s integration time with gain settings of 3600. Test samples were blank-corrected by subtracting BRET values to “no tracer control” BRET values. Data was presented and analyzed using the GraphPad Prism software.

Milli-BRET units (mBU) were calculated by the following equation:

$$mBU = [(Acceptor_{sample} \div Donor_{sample}) - (Acceptor_{no\text{-}tracer\ control} \div Donor_{no\text{-}tracer\ control})] \times 1000 \quad [1]$$

Tracer apparent affinities (EC_{50}) were determined by fitting the Tracer Titration results into a three-parameter non-linear regression curve and calculated by the following equation:

$$Y = Bottom + X*(Top - Bottom)/(EC_{50} + X) \quad [2]$$

Compound apparent affinity (IC_{50}) was then calculated by fitting the data into a three-parameter curve and determined using the following equation:

$$Y=Bottom + (Top – Bottom)/(1 + (X/IC_{50})) \quad [3]$$

4.8 Enzymatic assays

EcoDHFR enzymatic activity was monitored using the fluorescence generated by the enzyme-catalysed oxidation of NADPH in the presence of 7,8-dihydrofolate (diHF). All reactions were performed at 25 °C in reaction buffer containing 50 mM PIPES (pH 7.3), 0.05% Tween-20, 400 µM NADPH, 1.5 µM Bovine Serum Albumine (BSA) and 6.0 µM dithiothreitol (DTT) using flat bottom, low-volume, 384-well black plates (Corning; catalogue #3573). Enzyme reactions were started by the addition of 500 µM diHF to the reaction mixture and the NADPH fluorescence (excitation 340 nm / emission 445 nm) was collected using a BMG LABTECH Clariostar luminometer plate reader set on kinetic mode. To determine the optimal enzyme concentration for the assay, we followed reaction progress curves at increasing enzyme concentrations. All subsequent experiments were performed at the obtained half-maximal effective concentration (EC_{50}) for EcoDHFR (10 nM) and NLuc-EcoDHFR (13 nM). To estimate percent enzyme inhibition or half maximal inhibitory concentration (IC_{50}) values, compounds (antibiotics, TMP-derived fluorescent tracers, and test compounds) were first serially-diluted in 100% DMSO, and then either 0.002 µL or 0.1 µL of each compound was transferred to a 384-well plate containing the reaction buffer and the appropriate enzyme using the appropriate pin-tools in a CyBio FeliX liquid handler (Analytik Jena, Jena, Germany) (final DMSO concentrations in the assay were either 0.06% or 0.33%). Plates were incubated at 25 °C for 1 h and the reaction was started by the addition of diHF. Data was collected as above. Data was analyzed in MARS software (BMG Labtech) and both curve fitting and statistical analysis were performed in GraphPad Prism 7.

4.9 Microscopy

E. coli cells expressing the NanoLuc_EcoDHFR fusion protein were grown until the culture reached log phase. Cells were incubated with 1 µM of SV-97 tracer and 5 µg/mL of Hoescht DNA stain for 30 min at room temperature, and later fixed with 4% Paraformaldehyde on the slide.

Mounting media (ProLong Gold) was used to protect the tracer fluorescence from fading. Images were captured on a Leica TCS SP5 II Confocal Microscope using a X100 objective lens.

4.10 Viability assays

Bacterial cells were grown overnight in liquid media and diluted to an OD_{600} of 0.005 in fresh media. For the 1-point killing assay, 99 µL of culture was transferred to each well of a 96-well plate and 1µL of each test compound was added to a final concentration of 10 µM. For Minimum Inhibitory Concentration (MIC) assessments, compounds were serially diluted in 100% DMSO and 1 µL of each dilution point was transferred to the test plate containing 99 µL of the diluted overnight culture. Plates were incubated at 37 °C without shaking for 24 hours. Next, 10 µL of alamarBlue was added to the samples and incubated for 1 hour. The fluorescence intensity of each sample was measured in a BMG LABTECH Clariostar luminometer (excitation 560 nm / emission 590 nm).

4.11 Residence time assay

E. coli cells transformed with Nluc_EcoDHFR construct were grown to OD_{600} of approximately 0.7 and diluted 1:1 in warm M9 minimal media. Compounds were diluted to 100X in 100% DMSO, then diluted to 10X in M9 minimal media. 1.8 mL of diluted *E. coli* cells were incubated with 200 µL of the 10X compound for 1 hour at 37 °C. DMSO final concentration was 1%. Cells were then centrifuged at 35,000 r.p.m. for 5 min and supernatant was discarded to ensure that any extracellular compound was eliminated. 100 µL of diluted cell culture was transferred to a white, 96-well, flat-bottom, non-binding plate as above then 100 µL of a 2X concentrated cocktail containing NanoLuc substrate, Extracellular NanoLuc inhibitor and tracer (at a final concentration of 1 µM) were added immediately before reading the signal at the donor and acceptor wavelengths. Kinetic measurements were collected every two minutes for a total time of two hours (60 cycles) using a BMG LABTECH Clariostar luminometer with monochromator at 460-10 nm for BRET donor and a Long Pass (LP) 610-20 nm filter for BRET acceptor, 0.5 s integration time with gain settings of 3600.

5. Results and Discussion

5.1 Genetic engineering of wild-type and mutant BRET donor.

The donor in our energy transfer system is the NanoLuc luciferase fused with the target protein DHFR from *E. coli* (EcoDHFR). Both genes of interest were cloned into a pET-based expression vector, pNIC28-Bsa4[47], for episomal expression of the donor protein in *E. coli* cells. A major advantage of using pNIC28-Bsa4 was the Ligation-Independent cloning (LIC) site with a "stuffer" fragment that includes the sacB gene which encodes for the levansucrase enzyme, adding extra selection of the correct clones in the presence of sucrose, in addition of kanamycin, and a multiple cloning site which was used to introduce the second gene of interest into the vector. pNIC28-Bsa4 also has other useful features for this project, such as strong protein expression is driven by the T7-LacO system and a N-terminal His6-tag, important for purification of the recombinant protein for *in vitro* BRET assays (Figure 3).

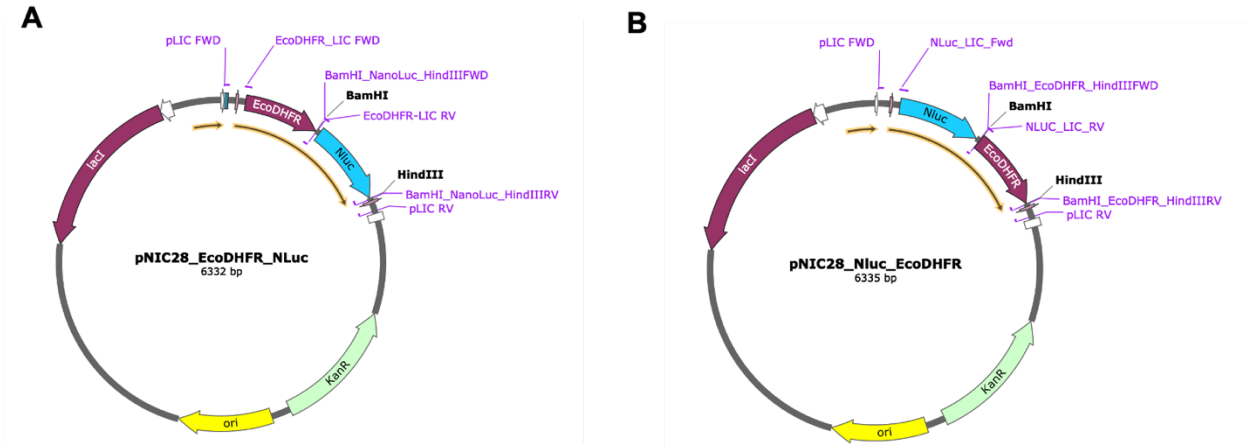

Figure 3- Overview of main features presented by expression vectors created for this study.

(A) pNIC28_EcoDHFR_Nluc **(B)** pNIC28_Nluc_EcoDHFR. Primers used in the cloning steps of the recombinant protein are indicated in purple. Expression vector maps were created using the software SnapGene.

We fused the NanoLuc to both C-terminal and N-terminal ends of EcoDHFR in order to evaluate if the position of NanoLuc in the fusion protein would have an impact the efficiency of the energy transfer. For the construction of C-terminal NanoLuc fusion, EcoDHFR was first

introduced into pNIC28-Bsa4 via LIC (Figure 4A), then NanoLuc was inserted in the C-terminal via restriction enzyme cloning (Figure 4B). For the construction of N-terminal NanoLuc fusion, NanoLuc was first introduced into pNIC28-Bsa4 via LIC (Figure 4C), then EcoDHFR was inserted in the C-terminal via restriction enzyme cloning (Figure 4D). The resulting constructs were verified by DNA sequencing after each cloning step using primers flanking annealing sites on the pNIC28-Bsa vector (pLIC).

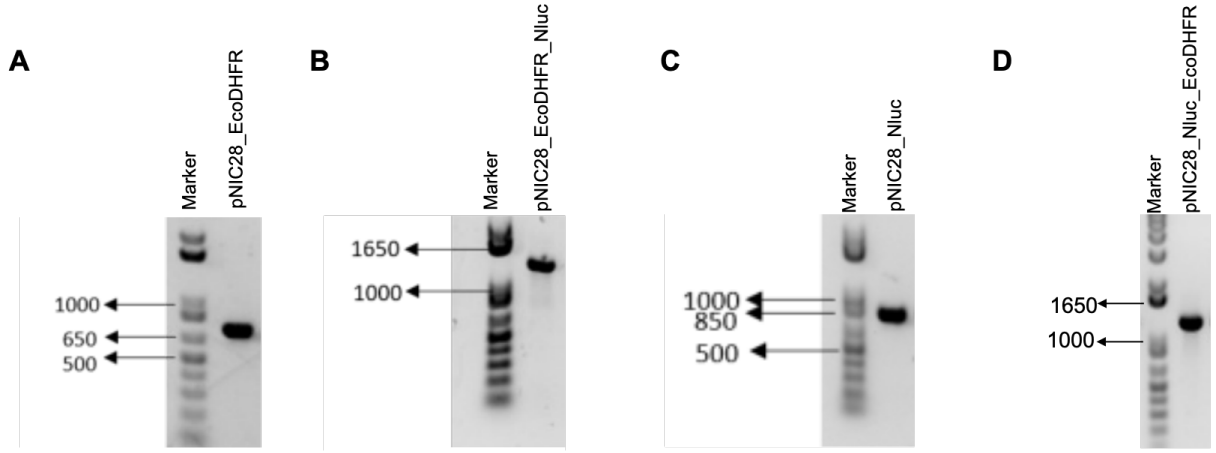

Figure 4- Colony PCR analysis after each cloning step.

1% agarose gel analysis to confirm the correct clone sizes prior to DNA sequencing **(A)** pNIC28_EcoDHFR 721 bp **(B)** pNIC_EcoDHFR_Nluc 1234 bp **(C)** pNIC28_Nluc 757 bp **(D)** pNIC28_Nluc_EcoDHFR 1237 bp. Molecular Marker: 1 Kb Plus DNA Ladder (Thermo Fisher Scientific).

Previous research has shown that a methionine to valine mutation at residue 20 (M20V) of EcoDHFR results in a significant loss of affinity between the enzyme and the antibiotic Trimetoprim[48]. Furthermore, this single-site mutation is important because it has been found in clinically isolated TMP-resistant *E. coli*. Creating a mutant version of the BRET donor would be particularly useful when evaluating the specificity of the TMP-based tracer with the EcoDHFR. We used the previously constructed pNIC28_Nluc_EcoDHFR vector as template to execute a one-step site-directed mutagenesis approach in order to create our BRET donor containing the M20V mutation in the EcoDHFR portion of the recombinant protein. For this approach, we created a set of primers that contained the desired mutation (ATG→GTG) and flanking the appropriate position

on the DNA. A PCR with this set of primers was used to amplify the entire vector followed by purification and transformation into *E. coli*. Multiple colonies were screened after transformation due to the lower success rate of the one-step site-directed mutagenizes method. The mutant BRET donor expression vector was confirmed by DNA sequencing (Figure 5).

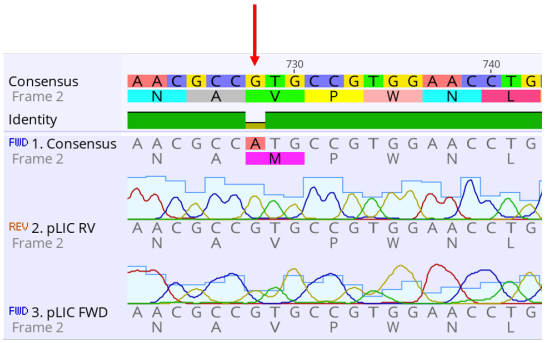

Figure 5- Electropherogram analysis to confirm the presence of the desired mutation.

Each peak represents a nitrogenous base (Adenine- red; Thymidine- green, Guanine- yellow and Cytosine- blue). The red arrow indicates where the mutation is located. The point mutation from a guanine to an adenine induced a switch of the amino acid valine to a methionine.

5.2 Production and purification of recombinant proteins

5.2.1 Small-Scale expression test

Once the sequences of the expression vectors were confirmed, they were transformed into *E. coli* BL21(DE3)-R3-pRARE2 with the intention of production and purification of the BRET donor for further *in vitro* BRET assays. The BL21(DE3) has been widely used for the high-level production of recombinant proteins as it carries the lambda DE3 prophage in its genomic DNA which encodes for the T7 RNA Polymerase whose expression can be induced by the addition of IPTG[49]. This feature is essential for the production of proteins whose genes are under control of the T7, such as ours.

Prior to executing large-scale protein purification, we tested the solubility of our recombinant proteins in small-scale protein purification (Figure 6). SDS-PAGE analysis of the tested samples EcoDHFR, EcoDHFR_Nluc and Nluc_EcoDHFR shows that all three were soluble

and suitable for a larger-scale protein purification. Furthermore, very little was lost in the wash step.

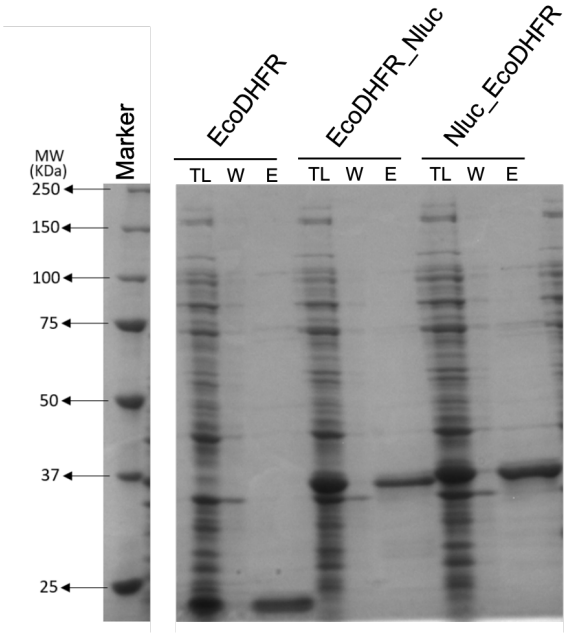

Figure 6- 10% SDS-PAGE analysis of small-scale expression test.

TL= Total Lysate, W= Wash, E=Elution**.** EcoDHFR-18KDa, EcoDHFR_Nluc-37 KDa and NanoLuc_EcoDHFR-37 kDA. Marker: Precision Plus Protein Standards (BioRad).

5.2.2 Large scale purification.

Next, we moved on to large-scale purification of the N-terminal and C-terminal NanoLuc fusions with EcoDHFR, NLuc_EcoDHFR and EcoDHFR_NLuc, as well as the mutant version of the BRET donor, NLuc_EcoDHFR(M20V), and EcoDHFR alone which was important for later enzymatic assays. Our recombinant proteins are expressed with a N-terminal tag composed of 6 histidine residues which binds to the nickel present in the IMAC column, allowing us to wash away proteins that do not have affinity for the column. Elution of the protein from the nickel column is achieved by competition with the imidazole present in the elution buffer. Later, we further purified our recombinant proteins using Size Exclusion Chromatography (SEC) which separates the molecules based on their size by filtration through a gel. Figure 7 shows the SDS-PAGE analysis of the IMAC elution of each sample and the Gel Filtration fractions collected after the purification steps.

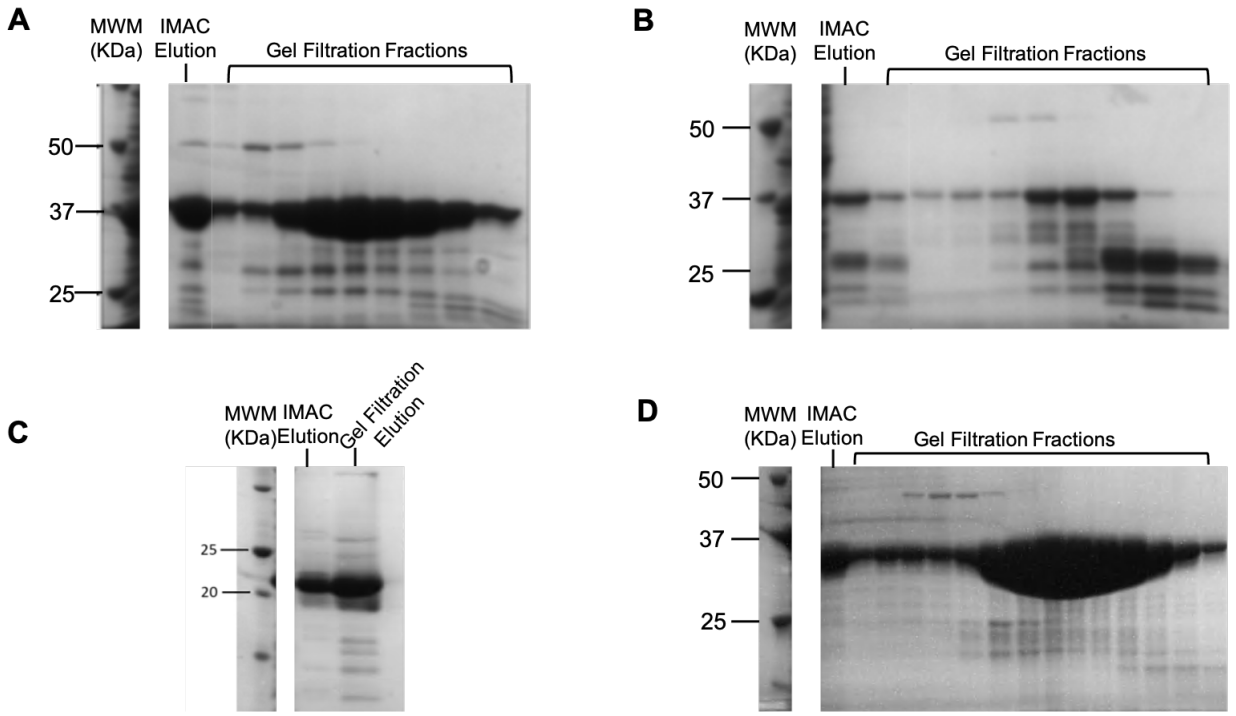

Figure 7– 10% SDS-PAGE analysis of large scale purification of recombinant proteins used in this work.

A) NanoLuc-_EcoDHFR- 40 KDa **B)** EcoDHFR_NanoLuc analysis shows low protein yield and impure protein **C)** EcoDHFR- 20 KDa **D)** NanoLuc-_EcoDHFR(M20V)- 40 KDa. Marker: Precision Plus Protein Standards (BioRad).

We were able to purify the recombinant proteins from the large-scale cultures and obtain high yields of NanoLuc_EcoDHFR (Figure 7A), EcoDHFR (Figure 7C) and NanoLuc_EcoDHFR(M20V) (Figure 7D). However, we could not recombinantly produce EcoDHFR_NanoLuc in sufficient quantities or purity for further *in vitro* assays (Figure 7B). It is possible that the C-terminal NanoLuc could have impaired the proper protein fold of the fusion protein or its binding to the IMAC column. Hence, all subsequent results were obtained using the NanoLuc N-terminal fusion protein. Successfully purified samples were further analyzed through LC-MS for confirmation of their correct size. We did not cleave the His-tag tag out as studies have shown that the tag does not have a significant impact on the structure of the protein[50].

5.3 Fusion protein retains both NanoLuc and EcoDHFR activities.

It was important for the success of the BRET experiment to verify if both components of our fusion protein retained their individual activities. NanoLuc utilizes furimazine as substrate to produce light with an emission peak at 460 nm. Addition of furimazine to purified NanoLuc_EcoDHFR resulted in light emission at the expected wavelength and the intensity of the emitted light was proportional to the amount of NanoLuc present in the assay, thus confirming that the luciferase component of the fusion protein was active (Figure 8).

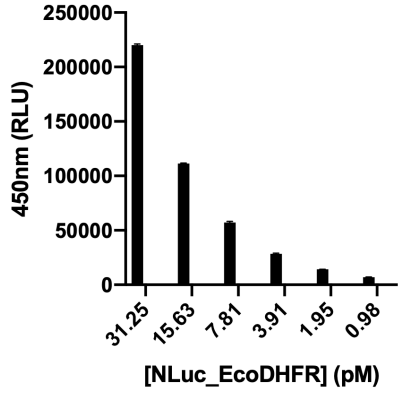

Figure 8- NanoLuc retains its activity when fused with EcoDHFR.

Addition of furimazine to purified NanoLuc_EcoDHFR resulted in concentration-dependent luminescence emission at 450 nm by the NanoLuc-catalyzed oxidation of furimazine.

DHFR utilizes NADPH as a cofactor to catalyze the reduction of dihydrofolic acid into tetrahydrofolic acid. This reaction can be followed by monitoring the decrease of NADPH fluorescence as it is oxidized to NADP by the enzyme in the presence of the substrate[51]. Using this enzymatic assay, we found similar EC_{50} values for both NanoLuc_EcoDHFR and EcoDHFR (11.3 nM and 10.9 nM, respectively) (Figure 9A). Moreover, when the same assay was executed in the presence of known DHFR inhibitors, here we used the clinically-approved drugs Trimethoprim and Methotrexate, equivalent IC_{50} values were found for both proteins (Figure 9B and C). All together, these results suggested that the presence of Nanoluc did not significantly alter the

enzymatic activity of EcoDHFR. Results shown in Figure 9B and C were executed by CQMED post-doctoral fellow Gustavo Riboldi.

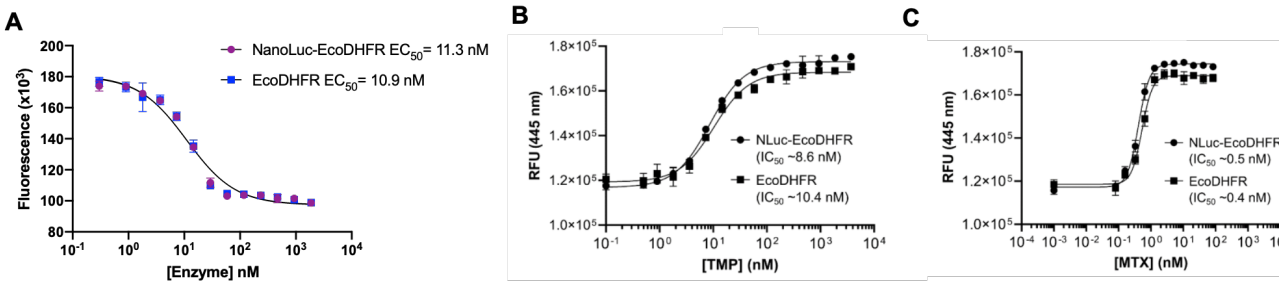

Figure 9- EcoDHFR retains its enzymatic activity when fused to NanoLuc

A) Enzymatic assay to calculate half-maximal effective concentrations (EC_{50}) for purified NanoLuc_EcoDHFR (purple circles) and EcoDHFR (blue squares). **B, C)** Determination of half-maximal inhibitory concentrations (IC_{50}) of **(B)** TMP and **(C)** MTX for purified EcoDHFR (black squares) and NanoLuc_EcoDHFR (black circles). Data shown in panels A-D were obtained by following the decay of the NADPH cofactor fluorescence as it is converted to NADP by the enzyme.

5.4 Creation of the BRET acceptor.

The second component of our BRET-based assay is the tracer. Ideally, this molecule should be capable of penetrating the cell envelope, reversibly bind to the EcoDHFR portion of the BRET donor, receive energy provided by the NanoLuc and, lastly, emit fluorescence of its own in a different wavelength. One possible way to create a molecule that meet these criteria is to modify a known ligand of the target protein by attaching a suitable fluorophore to it in a position that allows the energy transfer to occur between the NanoLuc and the fluorophore.

Dihydrofolate reductase (DHFR) is an enzyme present in all organisms and catalyzes the reduction of 7,8-dihydrofolate (diHF) to 5,6,7,8-tetrahydrofolate (THF), which is an essential component for the synthesis of purines, pyrimidines, and several amino acids. Because the DHFR is the only source of THF in the cell, its inhibition causes a blockage in the DNA synthesis pathway leading cell death.[52] Due to its essentiality, the DHFR has been a studied as a druggable target for many years and consequently plenty of data on this enzyme have been published, including its 3-D structure bound with the clinically-approved antibacterial drug Trimethoprim (TMP)[53]. Analysis of the crystal structure of the EcoDHFR-TMP complex reveled that TMP has structural features to be a good tracer candidate. For instance, the core of the TMP molecule is made of a 2,4-

diaminopyrimidine (DAP) moiety which has been shown to be crucial for a tight binding between the molecule and the active site of the enzyme. On the other side of the TMP molecule, there are three methoxy groups that would be amendable of modification for the attachment of the fluorophore, therefore interfering minimally with the binding of the TMP with the EcoDHFR (Figure 10A). The fluorophore attached to the TMP is a boron-based red-fluorescent dye with excitation wavelength of 576 nm e emission of 590 nm which fits the wavelengths required to be able to receive energy provided by the NanoLuc and emit fluorescence of its own. Two versions of the TMP-based tracer were synthesized for this study; SV-97 has a shorter linker between the TMP portion of the tracer and the fluorophore, while SV-96 has a longer linker (Figure 10B).

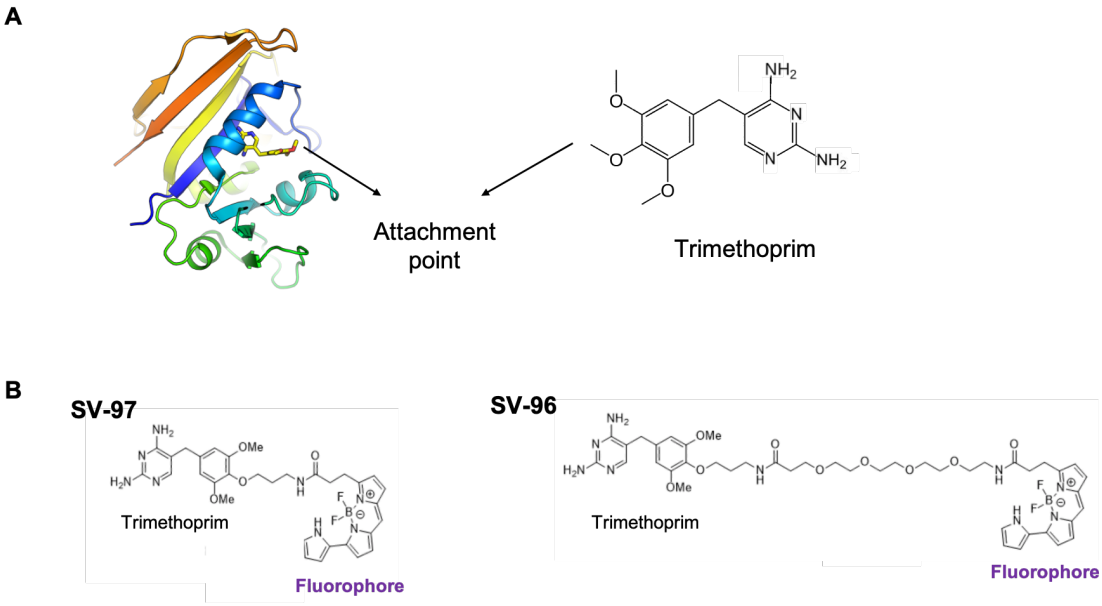

Figure 10- Design and creation of BRET acceptor

(A) Cristal structure of EcoDHFR-TMP complex and Trimethoprim structure with indication of modification point for the attachment of the fluorophore. 2,4-diaminopyrimidine is made of two amine groups on a pyrimidine ring, shown on the right side of the molecule. The fluorophore was attached to the portion of the molecule facing the solvent in order to be able to receive energy from the NanoLuc and interfere minimally with the binding of the TMP portion of the molecule and the enzyme. **(B)** Two versions of the TMP-based tracers developed at CQMED. The fluorophore used in this work is the BODIPY 576/589™ (Thermo Fisher Scientific).

5.5 BRET occurs with purified components and is donor-acceptor specific.

With both BRET components in hand, first we questioned whether BRET would occur between the NanoLuc_EcoDHFR and the TMP-based tracers *in vitro*. Following the addition of increasing amounts of the TMP-based tracers onto the purified NanoLuc_EcoDHFR and in the presence of NanoLuc substrate, furimazine, increasing mBU signals were recorded. When fitting these results into a dose-response curve, we estimated similar dissociation constants (K_d) for TMP-based tracers with short (SV-97, K_d = 30.8 nM) and long (SV-96, K_d = 39.5 nM) linkers indicating that the length of the linker does not significantly affect the binding and the energy transfer between BRET donor and acceptor (Figure 11A). On the other hand, repeating the experiment using a commercially available tracer that has the same fluorophore as our TMP-based tracer but was designed to bind to human kinases, no BRET signal was observed (Figure 11B). To further confirm the specificity of this interaction, we repeated the titration experiment using the mutant BRET donor, Nluc_EcoDHFR(M20V) and a ~ 3-fold reduction in affinity for the SV-97 tracer (K_d = 100.5 nM) (Figure 11C). Taken together, these results confirmed that BRET occurs following the specific interaction between donor and acceptor *in vitro* in a dose dependent manner.

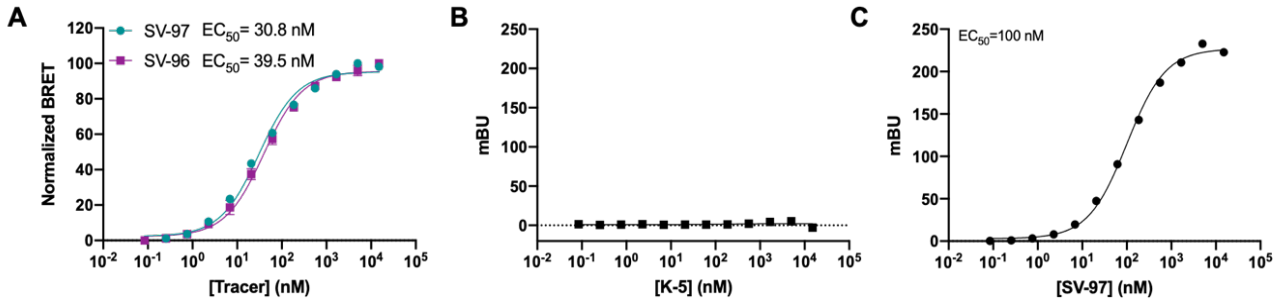

Figure 11- Tracer Titrations onto purified BRET donors.

A) Dose-response curve of TMP-based tracers developed at CQMED, SV-96 and SV-97 reveals that the length of the linker between the TMP portion of the molecule and the fluorophore does not significantly impair with the energy transfer between BRET donor and BRET acceptor and they present similar binding characteristics with the recombinant protein. **B)** Commercially available kinase K-5 tracer titration onto purified NanoLuc_EcoDHFR does not show BRET signal. **C)** SV-97 Tracer titration onto purified Mutant NanoLuc_EcoDHFR reveals weakened binding of the tracer with the BRET acceptor.

5.6 In cell BRET assays - protocol optimization.

5.6.1 NanoLuc substrate is cell-penetrant and NanoLuc Extracellular inhibitor assures intracellular BRET signal.

Once confident that the energy transfer between donor and acceptor was in fact possible *in vitro*, we moved on to perform similar experiments using living *E. coli* Bl21(DE3) cells. Similar to BRET *in vitro*, addition of furimazine into media containing *E. coli* cells expressing NanoLuc_EcoDHFR resulted in light emission at the expected wavelength. This occurred even without addition of the inducing agent IPTG to the medium, indicating "leaky" expression of the cloned gene. As expected, cells expressing EcoDHFR alone did not emit light following addition of furimazine to the medium. It is important for the success of the BRET assay to enssure that the observed BRET signal originates within cells. Even though the *E. coli* cells are minimally manipulated for these assays, cell lysis may occur and lead to the leakage of the BRET donor to the medium. For that reason, we tested a commercially available non-penetrant NanoLuc inhibitor[54] to be used in further BRET assays. When purified NanoLuc_EcoDHFR is added to media containing cells expressing EcoDHFR only, the extracellular NanoLuc inhibitor (NEI) is capable of reducing the extracellular NanoLuc signal by over 99%. When *E. coli* cells expressing the NanoLuc_EcoDHFR are compared between the addition of furimazine only and furimazine plus the extracellular NanoLuc inhibitor, the NanoLuc signal is only reduced by a small percentage, indicating that most of the emitted light comes from within the cells (Figure 12).

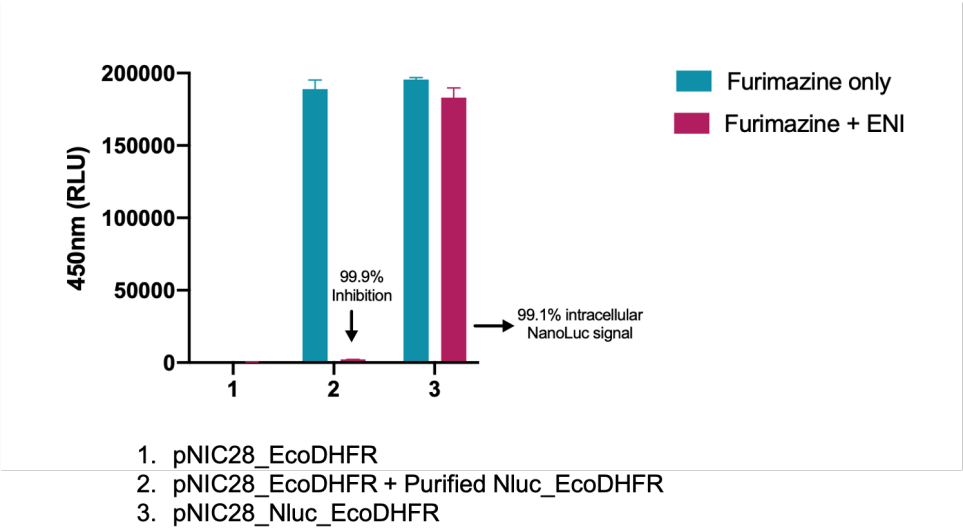

Figure 12- Extracellular NanoLuc inhibitor assessment.

Cells expressing plasmid pNIC28_EcoDHFR do not emit light at 450 nm in the presence of furimazine. Cells expressing pNIC28_EcoDHFR and in the presence of purified NanoLuc_EcoDHFR in the growth media emits lights at the expected wavelength in the presence of furimazine but the signal is attenuated when the Extracellular NanoLuc inhibitor (ENI) is added to the media. Cells expressing pNIC28_NanoLuc_EcoDHFR also emit lights at 450 nm in the presence of furimazine but only a small percentage of the signal is attenuated when the Extracellular NanoLuc inhibitor is added indicating that the majority of the observed signal is intracellular signal. Cells did not need to be induced with IPTG for the expression of the DHFR or NanoLuc_EcoDHFR

5.6.2 EcoDHFR retains its cellular function when fused to NanoLuc

To confirm that the DHFR portion of the donor protein also retained its original activity, we tested the TMP sensitivity of wild-type *E. coli* BL21(De3) cells and the same cells expressing NanoLuc_EcoDHFR. Our results showed that cells expressing the fusion protein were less sensitive to TMP due to the increased expression of functional DHFR (Figure 13A and B). These results confirmed that both enzymes making up the BRET donor were active and furimazine was cell-penetrant, whereas the NanoLuc extracellular inhibitor was not.

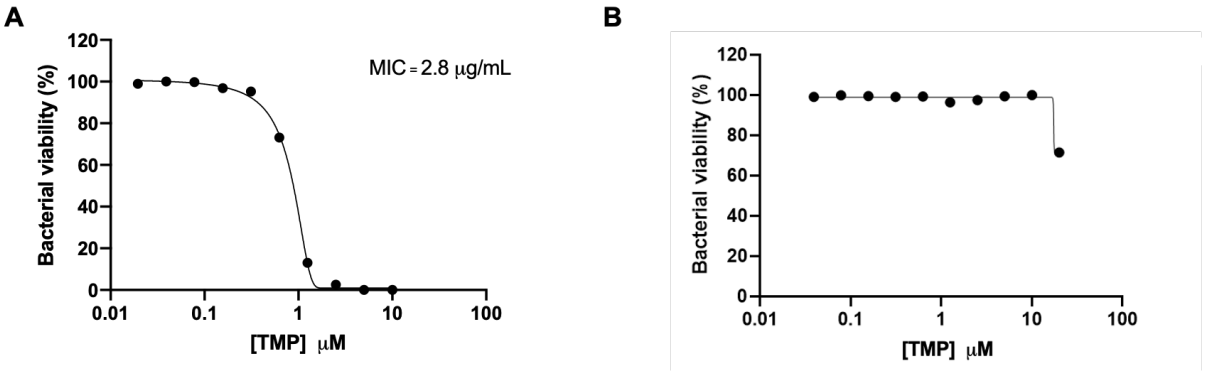

Figure 13- Trimethoprim (TMP) Minimum Inhibitory Concentration

for *E. coli* BL21(DE3) in the absence **(A)** and presence **(B)** of ectopic expression of NanoLuc_EcoDHFR. Cells become less sensitive to the TMP due to the higher expression of functional DHFR.

5.7 Tracer penetrates the bacterial cell envelope and BRET occurs in cells.

Gram-negative bacteria have a highly selective cell envelope; hence our next question was whether the TMP-based tracers would be able to penetrate the bacterial cell envelope, reach the cytoplasm and, finally, generate BRET. TMP alone is cell-penetrant in *E. coli* cells, but it was unclear if the attachment of the fluorophore to the TMP molecule would impair its cell permeability. Titration of tracer SV-97 onto live *E. coli* BL21(DE3) cells expressing NanoLuc_EcoDHFR resulted in a dose-response curve and allowed us to estimate a K_d value of 25.8 nM for this interaction, which was in excellent agreement with the results obtained using purified components (K_d = 30.8 nM). To confirm if the observed BRET signal resulted from the specific interaction between BRET donor and acceptor within living cells, we repeated these experiments using *E. coli* cells expressing the mutant BRET donor, which we showed had decreased binding to TMP *in vitro* (K_d = 100 nM). Indeed, in cells, the interaction between M20V EcoDHFR and TMP was reduced ~10-fold (K_d value of 275 nM) (Figure 14).

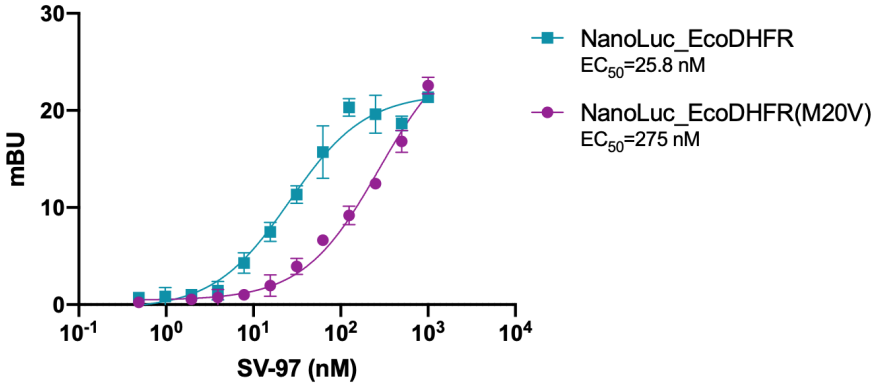

Figure 14- In cell Tracer Titration.

30-minute incubation of SV-97 into the bacterial cell culture medium results in specific and dose-dependent BRET measurements. *E. coli* BL21(DE3) cells expressing the mutant version of the recombinant protein (M20V) shows a weakened affinity with SV-97, consistent with the results obtained with the purified protein BRET assays.

To challenge these results, we performed two complementary experiments. First, we used confocal fluorescence microscopy to directly assess tracer accumulation within *E. coli* cells (Figure 15A). Second, we synthesized another TMP-based tracer (SV-235) having a positively charged and considerably bulkier fluorophore (Figure 15B). We expected these features to make the tracer less permeable to cells while retaining its ability to bind to EcoDHFR. Indeed, SV-235 showed similar EcoDHFR binding properties to the original tracer *in vitro* (K_d= 57.7 nM), but was considerably less active in living cells (K_d > 4,000 nM) (Figure 15C and D). Taken together, these findings suggested that BRET can be achieved within living *E. coli* cells and result from the specific interaction between intracellular NanoLuc-EcoDHFR and the tracer SV-97.

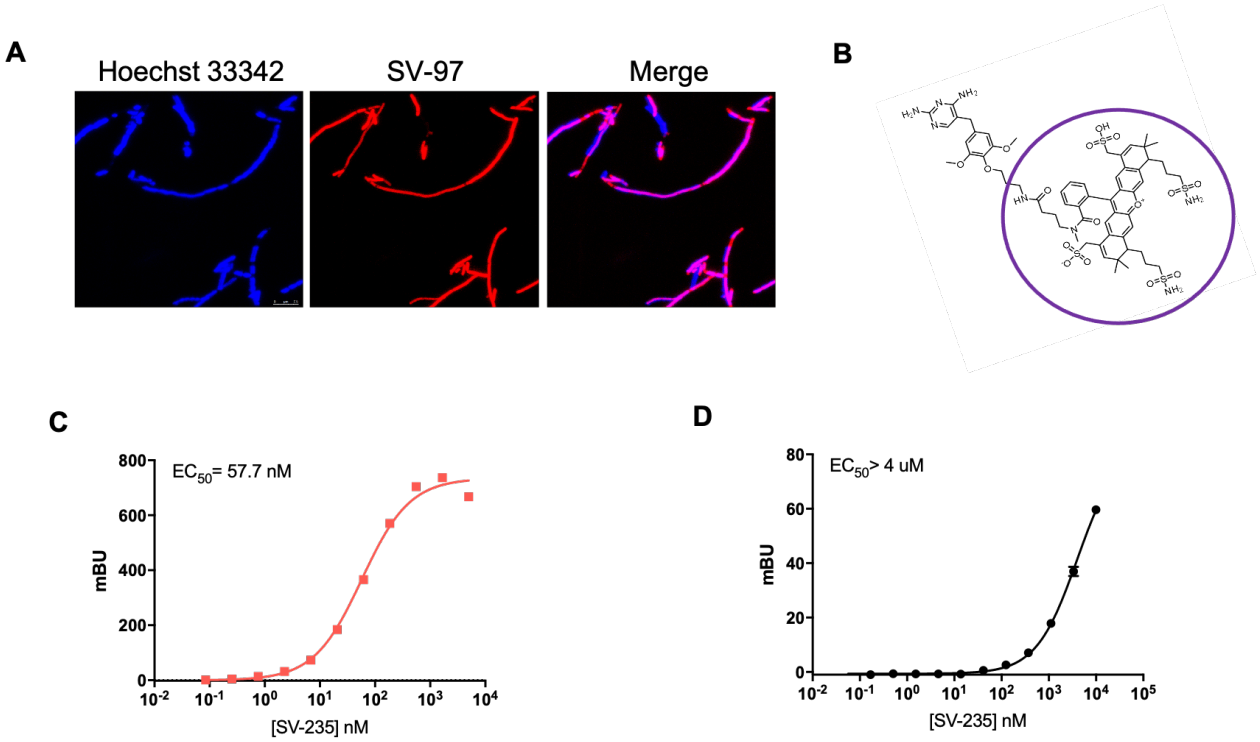

Figure 15- In cell Tracer permeability assessments.

A) Internalization of SV-97 by *E. coli* cells expressing NanoLuc_EcoDHFR analyses through confocal microscopy. **C)** Structure of non-penetrant TMP-based tracer SV-235. **C, D)** SV-235 titration onto purified NanoLuc_EcoDHFR **(C)** and onto cells expressing BRET donor **(D)**.

5.8 Competitive displacement of tracer causes loss of BRET signal

Next, we sought to ascertain that cell permeable ligands could competitively displace the TMP-based tracer from the BRET donor and disrupt, in a dose-dependent manner, BRET signal both *in vitro* and within living cells. For that, we used a fixed concentration of tracer (equivalent to the calculated EC_{80}) and titrated increasing amounts of unmodified, or "dark" TMP. Using purified protein *in vitro*, titrating increasing concentrations of TMP resulted in a proportional loss of BRET (K_d = 29.9 nM). Performing a similar experiment using *E. coli* BL21(DE3) cells expressing NanoLuc_EcoDHFR, we observed a similar dose-inhibition curve and a K_d of 8.9 nM (Figure 16).

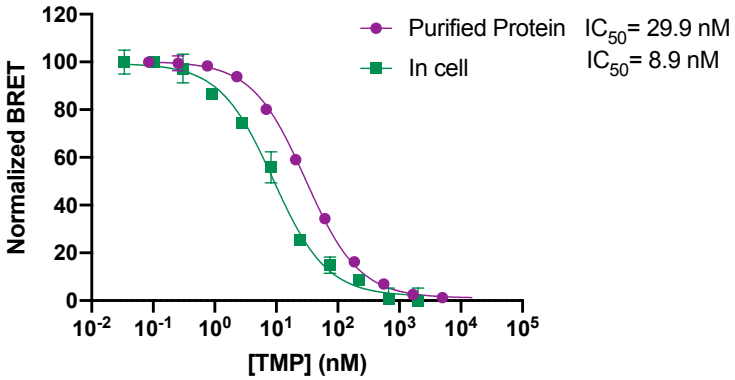

Figure 16- Tracer Displacement with unmodified TMP.

Attenuation of BRET signal by titration of TMP in the presence of TMP-based tracer SV-97 indicates the displacement of the tracer from the binding pocket of the intracellular NanoLuc_EcoDHFR leading to disruption of the energy transfer between BRET donor and BRET acceptor.

Similar to TMP, Methotrexate (MTX) is a folate analogue and extremely potent DHFR inhibitor often used as chemotherapeutic agent[55]. Titration of MTX onto the purified NanoLuc_EcoDHFR resulted in a significantly lower K_d (9.9 pM) compared to TMP, indicating a much higher affinity for the EcoDHFR (Figure 17A). However, in-cell titration of MTX showed very little displacement even when much higher concentrations were used (Figure 17B). This result, surprising at first, was consistent with previous observations as it is known that MTX is actively exported out of *E. coli* cells through the TolC dependent AcrAB efflux pump present in most laboratory strains of *E. coli*[56]. Thus, despite its potent *in vitro* activity, MTX does not accumulate within the cytoplasm of *E. coli* cells, making it an ineffective antibiotic against these bacteria. MIC assessment confirmed that our wild-type *E. coli* BL21(DE3) is not sensitive to MTX (Figure 17C). The tracer displacement assays presented above allow us to conclude that BRET can be used for the direct assessment of target engagement by cell permeable ligands within intact *E. coli* cells.

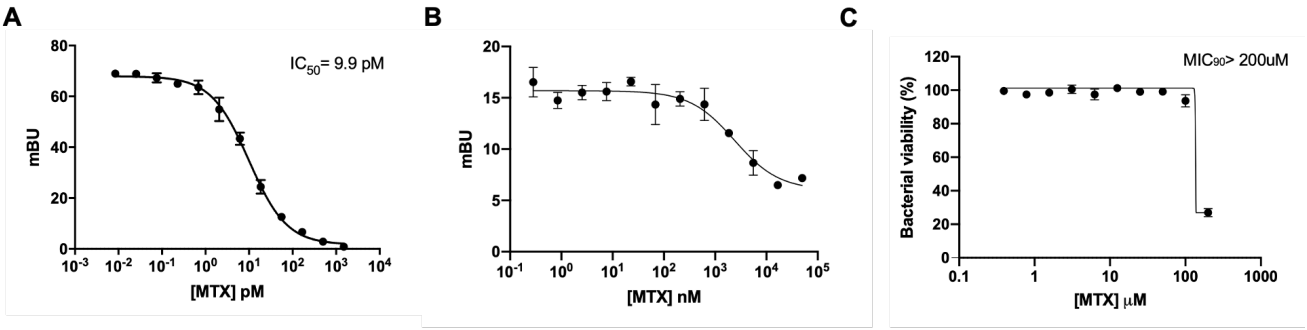

Figure 17- Tracer Displacement assay with Methotrexate.

A) MTX revels to have great *in vitro* potency but poor **(B)** in-cell potency. **C)** MTX Minimal inhibitory concentrations (MIC) for BL21(De3) *E. coli* cells.

5.8 Using BRET to evaluate drug intracellular residence.

Effective antibacterial compounds must, not only cross the bacterial cell envelope and engage with its target, but also reside within the cytoplasm long enough to disrupt essential cellular activities and cause cell death. Although it has been shown that *E. coli* cells become more sensitive to MTX when the TolC gene is inactivated by Tn10 insertion, it is unclear whether MTX in fact resides longer within the cell in the absence of the TolC. We used the TolC knockout strain from the Keio Collection single-gene knockout library and its parent strain BW25113 (wild-type) to investigate the residence time of MTX and TMP using the BRET system. The Keio Collection strains are derived from *E. coli* K-12, thus these cells do not express the T7 RNA polymerase required for the expression of the BRET donor in our previously constructed pNIC28_NanoLuc_EcoDHFR expression vector. Consequently, we cloned the entire NanoLuc_EcoDHFR cassette into an arabinose inducible expression vector, pBAD24 in order to obtain our BRET donor in these cells.

We confirmed the genotype of the TolC knockout and its parent strain through PCR using primers that are that are homologous to regions adjacent to the targeted gene. The Keio Collection single-gene knockout library was created using the λ Red system to substitute non-essential genes with a kanamycin resistance cassette[57], thus we confirmed that the parent strain still contained the TolC gene (1482 bp) and the TolC knockout presented a band size of the kanamycin resistance gene (1400 bp) (Figure 18A). We also sequenced the amplicons and

found that the TolC gene was present in parent strain and the kanamycin resistance gene was present in the TolC knockout. Next, we evaluated their sensitivity to TMP and MTX. As expected, the TolC knockout strain shows higher sensitivity for both drugs compared to the wild-type. Furthermore, BW25113 is not sensitive to MTX even at concentrations up to 45 µg/mL (Figure 18B).

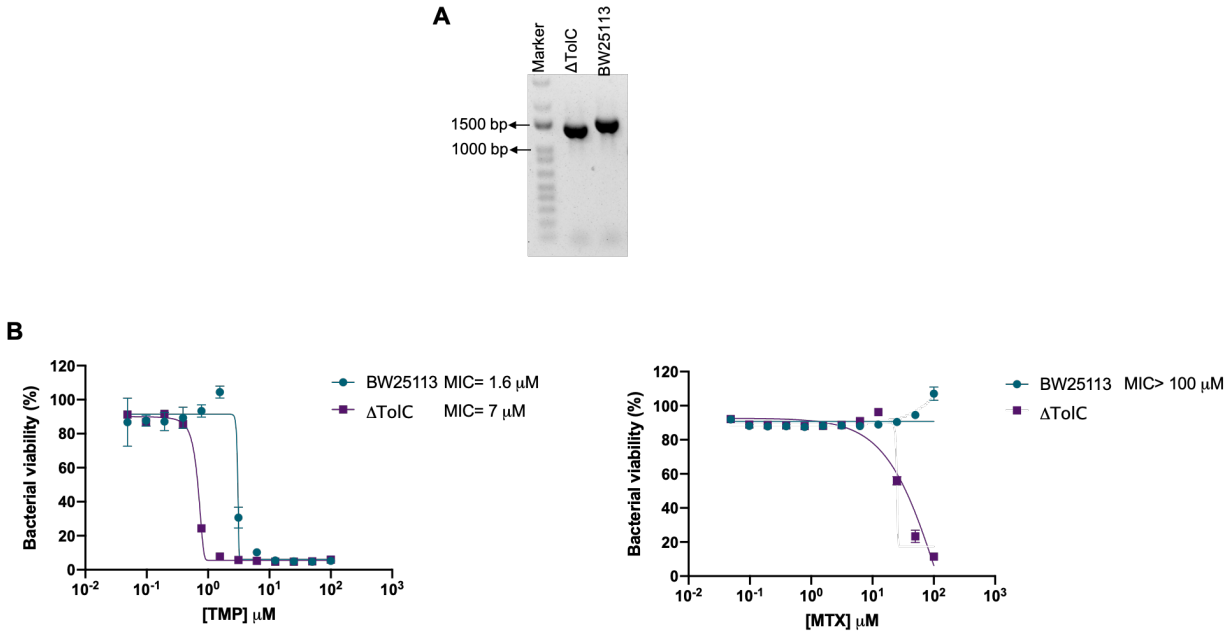

Figure 18- Validation of Keio Collection strains.

(A) Agarose gel. analysis of the PCR products to confirm the presence of the kanamycin resistance gene in the TolC knockout (1400 bp) and the TolC gene in the parent strain BW25113 (1482 bp). Molecular Marker: 1 Kb Plus DNA Ladder (Thermo Fisher Scientific). **(B)** Minimum inhibitory concentration (MIC) determination for Keio Collection strains with TMP and MTX.

Using the BRET approach to measure intracellular residence time of a drug consists of pre-treating the cells expressing the BRET donor with the compound for 2 hours so they can reach an equilibrium state, then any unbound compound is removed from the medium by a washing step, finally, a near-saturating concentration of the tracer is added and BRET is measured every two minutes over the course of two hours (Figure 19A). Addition of 400 nM of the SV-97 tracer to the cells expressing the NanoLuc_EcoDHFR without drug treatment (vehicle) resulted in a rapid increase in BRET signal until approximately the first

20 minutes, then steady BRET values are observed until the end of the readings for both cells, BW25113 and the ΔTolC. This is attributed to the time necessary for the tracer to cross the cell envelope and reach an equilibrium state.

For the parental strain, BW25113, the BRET measurements of the cells treated with MTX follow the behavior of non-treated cells, while the low BRET signals are observed in cells treated with TMP (Figure 19B). We have shown that MTX has high affinity for the EcoDHFR, however it did not accumulate within the cytoplasm, consequently the tracer was able to accumulate and generate BRET. TMP, on the other hand, kept its occupancy constant in the cell, therefore the tracer was not able to bind to the EcoDHFR and very little BRET is observed throughout the entire 120 minutes. In contrast, MTX was able to evade efflux due to the absence of TolC-dependent efflux pumps, accumulate within the cytoplasm of the TolC mutant cells and prevent some BRET from occurring (Figure 19C). These results demonstrated yet another utility of our BRET-based assay: measuring intracellular drug residence time.

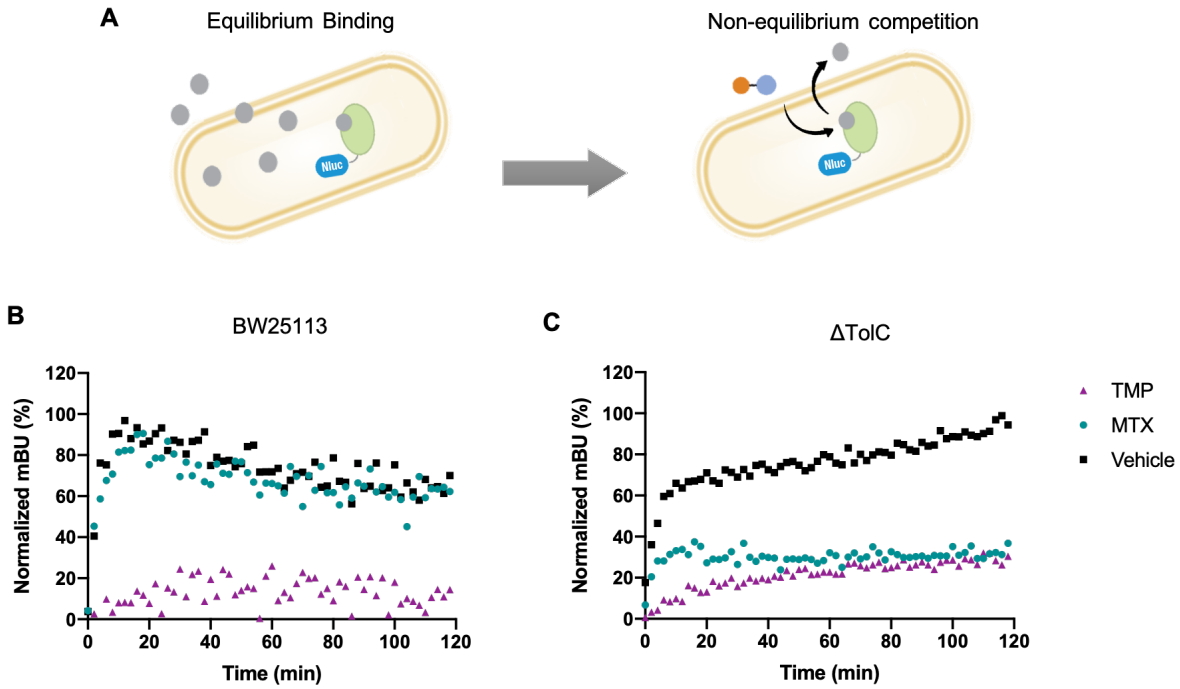

Figure 19- Measuring drug intracellular residence time using BRET.

(A) Overview of the assay used to measure MTX and TMP residence time. Cells were incubated with approximately MIC concentration of the drug for two hours, washed, then tracer was added immediately before BRET readings began. Compounds with longer residence time slow the production of BRET. Residence time analysis for TMP and MTX in **(B)** BW25113 and **(C)** ΔTolC cells from Keio Collection.

5.9 Tracer displacement reveals novel cell-penetrant DHFR ligands.

CQMED possesses a compound library composed of 175 compounds that were initially developed for *M. tuberculosis* DHFR but could be repurposed for *E. coli*. Some of these compounds exhibit a diaminopyrimidine (DAP) group in their structures, which is an interesting feature for EcoDHFR inhibitors. With that in mind, we used this compound library as means to demonstrate the utility of the BRET technology in finding new, cell-penetrant EcoDHFR ligands. First, we validated the tracer displacement assay in a 384-well plate format by titrating unmodified TMP in *E. coli* BL21(DE3) cells expressing the NanoLuc fused with EcoDHFR in the presence of the SV-97 tracer (Figure 20). We found an IC_{50} of 8 nM for the TMP which is in agreement with the value previously found in the 96-well format (IC_{50}= 8.9 nM). Furthermore, we found a Z' scored for this assay of 0.6, allowing us to conclude that this is a well suitable assay for higher-throughput format. Z'-Factor for our assays were estimated as described before [58].

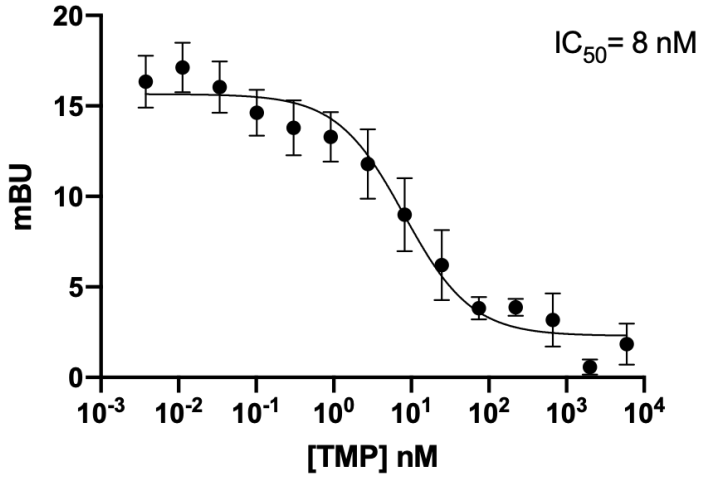

Figure 20-Validation of tracer displacement assay in a 384-well plate format

Titration of unmodified TMP onto cells expressing the BRET donor in the presence of a fixed concentration of tracer resulted in an equivalent IC_{50} value as previously found in 96-well plate format and good signal to background ration (z' score= 0.6).

Next, we used the 384-well plate format to perform a one-point tracer displacement assay, as well as a one-point enzymatic inhibition screen with the intention of evaluating permeability and

target engagement of the DHFR compound library. At 1.2 μM of compound we observed that 64.5% presented over 50% of enzymatic inhibition while only 44.5% of the entire library were able to displace over 50% of the tracer. This is expected because such compounds may not be cell-penetrant or they are expelled from the cytoplasm by the efflux-pumps, thus they cannot displace the tracer (Figure 21). Moreover, 10.9% of the compounds present less than 10% tracer displacement and less than 10% enzymatic inhibition, meaning that these compounds do not engage with the EcoDHFR. We found 5 compounds (O5, M5, A5, J4 and J2) that had less than 20% enzymatic inhibition but were relatively good ate displacing the tracer (>50% displacement). A possible explanation for this might be that these compounds could have been metabolized by the bacteria and gone through modifications that played in their advantage to have more affinity for the EcoDHFR therefore they display better in-cell activity. Another explanation could be that the intracellular environment could have favored the interaction of these compounds with the EcoDHFR, such as physiological concentration of the co-factor NADPH and Dihydrofolate or even the pH, though further investigation would be necessary to test these possibilities. Overall, these results indicate that BRET can be used to find new cell penetrant ligands for a given target protein from unbiased libraries in a high-throughput manner.

In-cell tracer displacement (%)

	1	2	3	4	5	6	7	8	9	10	11
A	103.3	82.9	74.0	65.2	59.0	46.6	27.3	17.4	-3.8	-23.7	-43.6
B	98.8	82.5	73.8	65.0	58.1	45.7	26.9	11.6	-5.4	-23.9	-44.2
C	98.3	82.5	73.5	64.8	56.2	45.0	24.8	11.6	-5.6	-25.9	-45.1
D	98.0	81.7	72.6	64.0	55.9	44.7	24.2	11.4	-6.4	-25.9	-45.7
E	97.6	80.8	71.6	64.0	55.8	43.3	23.4	9.9	-7.5	-27.6	-47.2
F	97.4	79.4	71.5	63.8	55.7	41.0	21.6	7.6	-9.5	-28.2	-47.3
G	93.8	79.1	70.8	63.6	55.2	40.9	21.3	4.9	-10.5	-31.3	-49.7
H	92.9	79.1	69.0	62.8	55.2	35.8	21.1	4.8	-11.9	-31.7	-49.9
I	89.0	78.8	68.5	62.7	54.8	35.3	19.7	3.2	-12.7	-32.1	-51.4
J	87.7	77.9	67.7	62.0	54.6	34.2	19.5	1.4	-14.3	-33.0	-52.6
K	85.9	77.9	67.6	61.6	53.8	33.8	19.4	0.9	-16.2	-35.0	-55.0
L	85.5	77.6	67.6	61.4	52.8	33.5	19.2	0.4	-19.9	-36.2	-57.7
M	85.4	76.3	67.4	61.4	52.3	31.6	19.0	-1.1	-20.3	-38.4	-58.3
N	85.0	75.2	66.4	61.1	51.7	30.3	18.6	-1.5	-20.5	-40.5	-67.7
O	84.7	74.6	65.9	60.6	49.6	30.0	17.7	-2.5	-22.1	-40.6	-67.9
P	84.0	74.1	65.6	59.4	47.2	29.9	17.6	-3.4	-23.0	-41.1	

100% 0%

***In vitro* enzymatic inhibition (%)**

	1	2	3	4	5	6	7	8	9	10	11
A	96.63	79.98	80.17	97.74	18.91	87.82	89.29	95.35	46.59	66.41	95.18
B	99.84	98.78	64.97	92.26	98.06	94.43	32.08	94.21	11.51	85.93	17.61
C	90.94	86.94	21.41	60.20	74.62	68.06	13.32	2.31	94.21	13.60	47.55
D	97.49	88.55	91.12	66.47	79.43	98.19	9.19	93.06	64.72	52.48	-1.20
E	97.98	57.13	96.53	92.79	44.93	83.28	5.60	11.07	2.53	92.57	3.90
F	93.25	89.21	91.01	88.29	94.06	84.07	84.54	3.51	89.75	7.44	4.33
G	96.51	90.91	91.09	74.26	70.34	15.15	92.38	9.90	10.42	46.94	8.50
H	74.95	98.68	91.08	89.93	59.94	60.03	51.82	54.92	20.18	39.80	0.17
I	96.57	96.07	81.16	68.64	92.19	8.83	6.05	10.06	90.54	7.77	86.95
J	96.55	12.39	71.78	15.18	62.22	64.91	17.74	81.26	78.52	37.30	8.63
K	92.26	100.00	93.79	69.03	76.84	18.32	32.39	83.75	58.29	52.45	15.40
L	94.14	76.59	94.84	81.35	98.56	49.61	2.56	79.18	11.04	23.45	6.52
M	49.90	93.31	58.51	87.51	14.46	89.67	58.84	78.74	6.96	78.81	0.65
N	95.18	93.33	90.67	98.83	59.94	97.18	80.15	9.56	17.87	79.37	13.60
O	95.38	90.86	93.29	38.27	5.24	10.26	77.94	67.73	16.86	27.07	6.68
P	96.00	81.10	78.77	80.14	40.32	64.80	9.02	57.07	13.76	22.49	

100% 0%

Figure 21- One-point in-cell tracer displacement vs. enzymatic inhibition.

High-throughput screening of 175 compounds from DHFR inhibitor library at 1.2 µM. Top panel: in-cell SV-96 tracer displacement assay. Bottom panel: *in vitro* EcoDHFR enzymatic inhibition.

5.10 BRET can be expanded to other pathogens.

Once established in *E. coli*, we worked on demonstrating the possibility of transferring the BRET technology to other pathogenic organisms. Mycobacteria have a cell envelope made up mainly of mycolic acids, and are known to have a large number of efflux pumps[59,60]. These characteristics make the permeability and accumulation of small molecules in these organisms even more difficult. With that in mind, we used the same cloning methods to produce a BRET donor, but this time using DHFR from *Mycobacterium abscessus* (Mabs) as the target protein and the expression vector pMV306hsp, used for

genome integration at the attP/B site of the Mabs genome. We verified the expression and activity of the fusion protein by adding the NanoLuc substrate, furimazine, into the culture medium and observed a robust signal at the expected wavelength (Figure 22A). As in *E. coli*, titration of the same TMP-based tracer SV-97 used in previous essays, allowed us to calculate an apparent K_d for the interaction between NanoLuc_MabsDHFR and the tracer, in cell, of 438 nM, (Figure 22B) which allowed us to continue and use BRET to test new compounds against the MabsDHFR. We then, performed the tracer displacement assay and identified three cell-penetrant compounds that interact with the target protein, SDDC-1248, SDDC-1567 and SDDC-1249 (Figure 22C). Although these compounds are not as potent as TMP, for example, they can serve as starting points for new small molecule chemical series that could display higher potency against MabsDHFR.

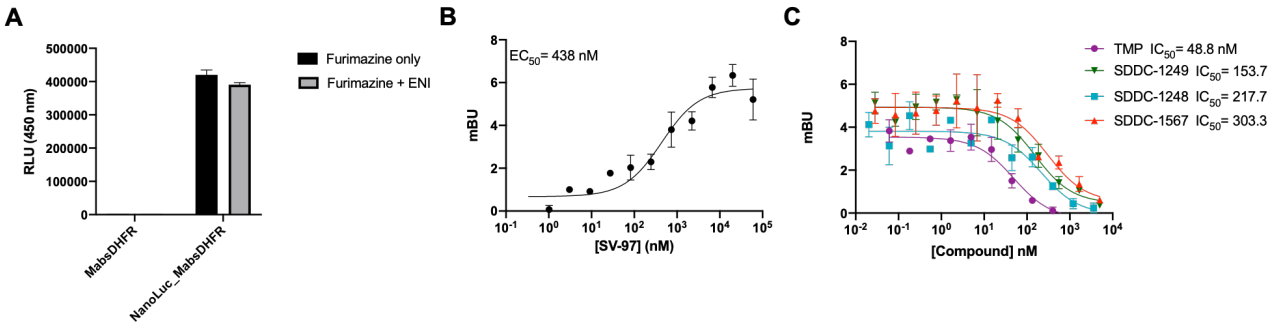

Figure 22- BRET development in M. abscessus.

A) Addition of furimazine to *M. abscessus* culture media results in luminescence emission at 450 nm for cell expressing the fusion protein NanoLuc_MabsDHFR while no luminescence is observed in cells expressing only the MabsDHFR portion of the BRET donor. **B)** TMP-based tracer SV-97 used in *E. coli* BRET assays is permeable in *M. abscessus* cells and binds to MabsDHFR thus generating BRET. **C)** Cell-penetrant SDDC compounds rank-ordered by affinity with NanoLuc_MabsDHFR measured through BRET tracer displacement.

6. Conclusions and perspectives.

Bacterial resistance is the "Achilles' heel" of the development of antibiotics. It only takes about two years after a new antimicrobial enters the market before bacteria can acquire resistance to the drug. This means that efforts to develop and discover new antimicrobials to counterbalance of the emergency of resistant microorganisms is a never-ending task. Though very successful in 1940-1960s, only a few antimicrobial drugs have been marketed with new mechanisms of action since then. Part of the reason is attributed to the fact that the pharmaceutical companies still pursuing antibiotic discovery have been focusing mainly on analog development. This approach is advantageous because analogues tend to exhibit similar important characteristics to their parent structure, such as solubility and toxicity levels. However, a major drawback is that there are limited number of modifications that can be made to a compound's core structure and some classes of antibiotics are more easily modified than others; as an example, cephalosporins, penicillins and quinolones have had more analogues brought to market than other classes of antibiotics. On the other hand, screening for novel and unique compounds is harder and riskier in a sense that most "easy-to-find" compounds may have already been discovered and there is a limited number of essential molecular targets and mechanisms of action associated with an organism. To this end, the antimicrobial discovery and development pipeline could benefit a lot from innovative ways to screen small molecules for precedented targets in bacteria.

In the work presented hereby, we developed a Bioluminescence Resonance Energy Transfer (BRET)-based assay in bacterial cells that combines the strengths of both of the most commonly used compound screening methods, in-cell and target engagement. The bacBRET allows us to evaluate the engagement of a molecular target with an antibiotic candidate. A particularly important characteristic of this assay is that it is executed with minimally manipulated live cells and close to physiological conditions. This assay has demonstrated to be very useful for screening compound libraries, analogues or not, with the intention of finding new cell permeable ligands for a given target. Moreover, there are other important questions that the bacBRET can answer about a given compound, for example, measuring its intracellular residence time and conducting small-molecule permeability studies by comparing the compound's ability to displace the tracer *in vitro* and in-cell, thus generating knowledge on what physical-chemical properties a compound should have in order to be a good drug candidate. The answers derived from the different applications of the

bacBRET assays are valuable assets that can aid and speed up the design and discovery of new chemical structures that can eventually become an antimicrobial drug.

Even though the bacBRET can bypass some of the common obstacles presented by the classic phenotype-based assays and the target-based assays used in the antibiotic discovery pipeline, for example, finding the mechanism of action of compounds with good in-cell activity or predicting whether a compound with good *in vitro* activity will be permeable or not, it does have some limitations; (i) bacBRET requires some previous structural knowledge of the target protein in order to become a BRET donor, (ii) bacBRET also requires at least one known ligand of the target protein and this ligand has to be suitable for structural modification for the attachment of the fluorophore to become the BRET acceptor (iii) the Nanoluc substrate and extracellular inhibitor cocktail makes the bacBRET a relatively expensive assay when compared to other traditional assays. For instance, the Nanoluc substrate and extracellular inhibitor cocktail costs $1.21 US dollars per reaction, while the ADP-Glo, an assay used for compound primary screening in purified kinases, costs only $0.4 US dollars. Though we hope that the BRET-based assays become widely used for other pathogens and molecular targets, and drive the price down for these consumables.

Antibiotic discovery currently faces major challenges that need to be addressed in order to circumvent another major public health crisis related to infectious diseases. Innovations, such as bacBRET, are important steps towards fighting bacterial resistance, but other measurements must be put in action. First, antibiotics should be used less abundantly or using an antibiotic combination therapy approach should reduce the rate of resistance emergency. Secondly, local governments should provide financial support such as tax incentives, grants and subsides for pharmaceutical companies and academia to encourage their return to the antibiotic discovery research. Charging higher prices for these drugs is one way to make reduce their unnecessary use and make them more attractive and profitable for the pharmaceutical companies. Lastly, loosening regulatory requirements may bring down the costs associated with developing these drugs. Together, we can overcome the emergence of resistance one microbe at a time.

7. Bibliography

1. Hutchings M, Truman A, Wilkinson B. Antibiotics: past, present and future. *Curr Opin Microbiol*. 2019;51:72-80. doi:10.1016/j.mib.2019.10.008

2. Lewis K. Platforms for antibiotic discovery. *Nat Rev Drug Discov*. 2013;12(5):371-387. doi:10.1038/nrd3975

3. Payne DJ, Gwynn MN, Holmes DJ, Pompliano DL. Drugs for bad bugs: Confronting the challenges of antibacterial discovery. *Nat Rev Drug Discov*. 2007;6(1):29-40. doi:10.1038/nrd2201

4. WHO. *Global Priority List of Antibiotic-Resistant Batceria to Guide Research, Discovery, and Development of New Antibiotics*.; 2017.

5. Silver LL. Challenges of antibacterial discovery. *Clin Microbiol Rev*. 2011;24(1):71-109. doi:10.1128/CMR.00030-10

6. Monserrat-Martinez A, Gambin Y, Sierecki E. Thinking outside the bug: Molecular targets and strategies to overcome antibiotic resistance. *Int J Mol Sci*. 2019;20(6). doi:10.3390/ijms20061255

7. Swinney DC. Phenotypic vs. Target-based drug discovery for first-in-class medicines. *Clin Pharmacol Ther*. 2013;93(4):299-301. doi:10.1038/clpt.2012.236

8. Tommasi R, Brown DG, Walkup GK, Manchester JI, Miller AA. ESKAPEing the labyrinth of antibacterial discovery. *Nat Rev Drug Discov*. 2015. doi:10.1038/nrd4572

9. Crick FHC, Barnett L, Brenner S, Watts-Tobin RJ. General nature of the genetic code for proteins. *Nature*. 1961. doi:10.1038/1921227a0

10. Nirenberg M, Leder P, Bernfield M, et al. RNA codewords and protein synthesis, VII. On the general nature of the RNA code. *Proc Natl Acad Sci U S A*. 1965. doi:10.1073/pnas.53.5.1161

11. KORNBERG A. Enzymatic synthesis of deoxyribonucleic acid. *Harvey Lect*. 1957. doi:10.1016/s0022-2836(65)80058-4

12. Jacob F, Monod J. Genetic regulatory mechanisms in the synthesis of proteins. *J Mol Biol*. 1961. doi:10.1016/S0022-2836(61)80072-7

13. Cohen SN, Chang ACY, Boyer HW, Helling RB. Construction of biologically functional bacterial plasmids in vitro. *Proc Natl Acad Sci U S A*. 1973. doi:10.1073/pnas.70.11.3240

14. Chen X, Zhou L, Tian K, et al. Metabolic engineering of Escherichia coli: A sustainable industrial platform for bio-based chemical production. *Biotechnol Adv*. 2013. doi:10.1016/j.biotechadv.2013.02.009

15. Jullesson D, David F, Pfleger B, Nielsen J. Impact of synthetic biology and metabolic engineering on industrial production of fine chemicals. *Biotechnol Adv*. 2015. doi:10.1016/j.biotechadv.2015.02.011

16. Adamczyk PA, Reed JL. Escherichia coli as a model organism for systems metabolic engineering. *Curr Opin Syst Biol*. 2017. doi:10.1016/j.coisb.2017.11.001

17. Smillie C, Garcillán-Barcia MP, Francia MV, Rocha EPC, de la Cruz F. Mobility of Plasmids. *Microbiol Mol Biol Rev*. 2010. doi:10.1128/mmbr.00020-10

18. Baba T, Ara T, Hasegawa M, et al. Construction of Escherichia coli K-12 in-frame, single-gene knockout mutants: The Keio collection. *Mol Syst Biol*. 2006. doi:10.1038/msb4100050

19. Hartl DL, Dykhuizen DE. The population genetics of Escherichia coli. *Annu Rev Genet*. 1984. doi:10.1146/annurev.ge.18.120184.000335

20. Bruyand M, Mariani-Kurkdjian P, Hello S Le, et al. Paediatric haemolytic uraemic syndrome related to Shiga toxin producing Escherichia coli, an overview of 10 years of surveillance in France, 2007 to 2016. *Eurosurveillance*. 2019. doi:10.2807/1560-7917.ES.2019.24.8.1800068

21. Karch H, Denamur E, Dobrindt U, et al. The enemy within us: Lessons from the 2011 European Escherichia coli O104:H4 outbreak. *EMBO Mol Med*. 2012. doi:10.1002/emmm.201201662

22. Cassini A, Högberg LD, Plachouras D, et al. Attributable deaths and disability-adjusted life-years caused by infections with antibiotic-resistant bacteria in the EU and the European Economic Area in 2015: a population-level modelling analysis. *Lancet Infect Dis*. 2019. doi:10.1016/S1473-3099(18)30605-4

23. Silhavy TJ, Kahne D, Walker S. The Bacterial Cell Envelope1 T. J. Silhavy, D. Kahne and S. Walker, . *Cold Spring Harb Perspect Biol*. 2010. doi:10.1101/cshperspect.a000414

24. Vollmer W, Blanot D, De Pedro MA. Peptidoglycan structure and architecture. *FEMS Microbiol Rev*. 2008. doi:10.1111/j.1574-6976.2007.00094.x

25. Amaral L, Martins A, Spengler G, Molnar J. Efflux pumps of Gram-negative bacteria: What they do, how they do it, with what and how to deal with them. *Front Pharmacol*. 2014. doi:10.3389/fphar.2013.00168

26. Nakae T. Identification of the outer membrane protein of E. coli that produces transmembrane channels in reconstituted vesicle membranes. *Biochem Biophys Res Commun*. 1976. doi:10.1016/0006-291X(76)90913-X

27. Koebnik R, Locher KP, Van Gelder P. Structure and function of bacterial outer membrane proteins: Barrels in a nutshell. *Mol Microbiol*. 2000. doi:10.1046/j.1365-2958.2000.01983.x

28. Fralick JA. Evidence that TolC is required for functioning of the Mar/AcrAB efflux pump of Escherichia coli. *J Bacteriol*. 1996. doi:10.1128/jb.178.19.5803-5805.1996

29. Borges-Walmsley MI, McKeegan KS, Walmsley AR. Structure and function of efflux pumps that confer resistance to drugs. *Biochem J*. 2003. doi:10.1042/BJ20020957

30. Mortimer PGS, Piddock LJV. A comparison of methods used for measuring the accumulation of quinolones by enterobacteriaceae, pseudomonas aeruginosa and staphylococcus aureus. *J Antimicrob Chemother*. 1991. doi:10.1093/jac/28.5.639

31. Cai H, Rose K, Liang LH, Dunham S, Stover C. Development of a liquid chromatography/mass spectrometry-based drug accumulation assay in Pseudomonas aeruginosa. *Anal Biochem*. 2009. doi:10.1016/j.ab.2008.10.041

32. Davis TD, Gerry CJ, Tan DS. General platform for systematic quantitative evaluation of small-molecule permeability in bacteria. *ACS Chem Biol*. 2014. doi:10.1021/cb5003015

33. Poole K. Efflux-mediated resistance to fluoroquinolones in gram-negative bacteria. *Antimicrob Agents Chemother*. 2000. doi:10.1128/AAC.44.9.2233-2241.2000

34. Vaara M. Agents that increase the permeability of the outer membrane. *Microbiol Rev*. 1992. doi:10.1128/mmbr.56.3.395-411.1992

35. Sahalan AZ, Dixon RA. Role of the cell envelope in the antibacterial activities of polymyxin B and polymyxin B nonapeptide against Escherichia coli. *Int J Antimicrob Agents*. 2008. doi:10.1016/j.ijantimicag.2007.10.005

36. Weiss RL. Protoplast formation in Escherichia coli. *J Bacteriol*. 1976. doi:10.1128/jb.128.2.668-670.1976

37. Machleidt T, Woodroofe CC, Schwinn MK, et al. NanoBRET-A Novel BRET Platform for the Analysis of Protein-Protein Interactions. *ACS Chem Biol*. 2015. doi:10.1021/acschembio.5b00143

38. Pfleger KDG, Seeber RM, Eidne KA. Bioluminescence resonance energy transfer (BRET) for the real-time detection of protein-protein interactions. *Nat Protoc*. 2006. doi:10.1038/nprot.2006.52

39. Stoddart LA, Johnstone EKM, Wheal AJ, et al. Application of BRET to monitor ligand binding to GPCRs. *Nat Methods*. 2015. doi:10.1038/nmeth.3398

40. Robers MB, Dart ML, Woodroofe CC, et al. Target engagement and drug residence time can be observed in living cells with BRET. *Nat Commun*. 2015;6(May). doi:10.1038/ncomms10091

41. Wells CI, Vasta JD, Corona CR, et al. Quantifying CDK inhibitor selectivity in live cells. *Nat Commun*. 2020. doi:10.1038/s41467-020-16559-0

42. Pfleger KDG, Eidne KA. Illuminating insights into protein-protein interactions using bioluminescence resonance energy transfer (BRET). *Nat Methods*. 2006. doi:10.1038/nmeth841

43. Dacres H, Dumancic MM, Horne I, Trowell SC. Direct comparison of fluorescence- and bioluminescence-based resonance energy transfer methods for real-time monitoring of thrombin-catalysed proteolytic cleavage. *Biosens Bioelectron*. 2009. doi:10.1016/j.bios.2008.07.021

44. Hall MP, Unch J, Binkowski BF, et al. Engineered luciferase reporter from a deep sea

shrimp utilizing a novel imidazopyrazinone substrate. *ACS Chem Biol*. 2012. doi:10.1021/cb3002478

45. Schaub FX, Reza MS, Flaveny CA, et al. Fluorophore-NanoLuc BRET reporters enable sensitive In Vivo optical imaging and flow cytometry for monitoring tumorigenesis. *Cancer Res*. 2015. doi:10.1158/0008-5472.CAN-14-3538

46. Eschenfeldt WH, Lucy S, Millard CS, Joachimiak A, Mark ID. A family of LIC vectors for high-throughput cloning and purification of proteins. *Methods Mol Biol*. 2009. doi:10.1007/978-1-59745-196-3_7

47. Savitsky P, Bray J, Cooper CDO, et al. High-throughput production of human proteins for crystallization: The SGC experience. *J Struct Biol*. 2010. doi:10.1016/j.jsb.2010.06.008

48. Watson M, Liu JW, Ollis D. Directed evolution of trimethoprim resistance in Escherichia coli. *FEBS J*. 2007;274(10):2661-2671. doi:10.1111/j.1742-4658.2007.05801.x

49. Jeong H, Kim HJ, Lee SJ. Complete genome sequence of Escherichia coli strain BL21. *Genome Announc*. 2016. doi:10.1128/genomeA.00134-15

50. Carson M, Johnson DH, McDonald H, Brouillette C, DeLucas LJ. His-tag impact on structure. *Acta Crystallogr Sect D Biol Crystallogr*. 2007. doi:10.1107/S0907444906052024

51. Hawser S, Lociuro S, Islam K. Dihydrofolate reductase inhibitors as antibacterial agents. *Biochem Pharmacol*. 2006. doi:10.1016/j.bcp.2005.10.052

52. Kompis IM, Islam K, Then RL. DNA and RNA synthesis: Antifolates. *Chem Rev*. 2005. doi:10.1021/cr0301144

53. Cammarata M, Thyer R, Lombardo M, et al. Characterization of trimethoprim resistant: E.

coli dihydrofolate reductase mutants by mass spectrometry and inhibition by propargyl-linked antifolates. *Chem Sci*. 2017;8(5):4062-4072. doi:10.1039/c6sc05235e

54. Walker JR, Hall MP, Zimprich CA, et al. Highly Potent Cell-Permeable and Impermeable NanoLuc Luciferase Inhibitors. *ACS Chem Biol*. 2017. doi:10.1021/acschembio.6b01129

55. Raimondi MV, Randazzo O, Franca M La, et al. DHFR inhibitors: Reading the past for discovering novel anticancer agents. *Molecules*. 2019. doi:10.3390/molecules24061140

56. Kopytek SJ, Dyer JCD, Knapp GS, Hu JC. Resistance to methotrexate due to AcrAB-dependent export from Escherichia coli. *Antimicrob Agents Chemother*. 2000. doi:10.1128/AAC.44.11.3210-3212.2000

57. Datsenko KA, Wanner BL. One-step inactivation of chromosomal genes in Escherichia coli K-12 using PCR products. *Proc Natl Acad Sci U S A*. 2000. doi:10.1073/pnas.120163297

58. Zhang JH, Chung TDY, Oldenburg KR. A simple statistical parameter for use in evaluation and validation of high throughput screening assays. *J Biomol Screen*. 1999;4(2):67-73. doi:10.1177/108705719900400206

59. Dulberger CL, Rubin EJ, Boutte CC. The mycobacterial cell envelope — a moving target. *Nat Rev Microbiol*. 2020. doi:10.1038/s41579-019-0273-7

60. Vincent AT, Nyongesa S, Morneau I, Reed MB, Tocheva EI, Veyrier FJ. The mycobacterial cell envelope: A relict from the past or the result of recent evolution? *Front Microbiol*. 2018. doi:10.3389/fmicb.2018.02341

8. Annexes

8.1 Declaração de bioética e biossegurança

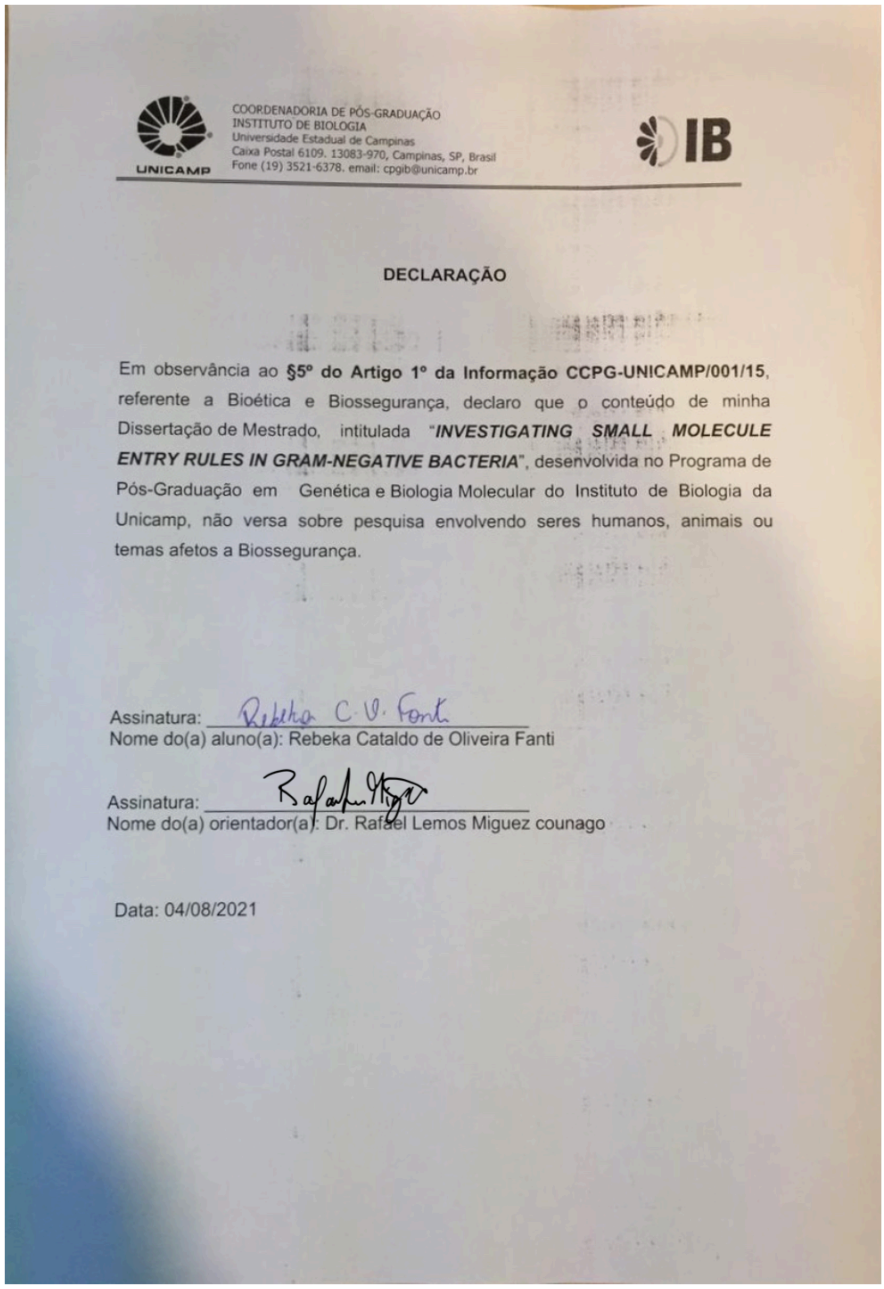

UNICAMP

COORDENADORIA DE PÓS-GRADUAÇÃO
INSTITUTO DE BIOLOGIA
Universidade Estadual de Campinas
Caixa Postal 6109. 13083-970, Campinas, SP, Brasil
Fone (19) 3521-6378. email: cpgib@unicamp.br

IB

DECLARAÇÃO

Em observância ao **§5º do Artigo 1º da Informação CCPG-UNICAMP/001/15**, referente a Bioética e Biossegurança, declaro que o conteúdo de minha Dissertação de Mestrado, intitulada "***INVESTIGATING SMALL MOLECULE ENTRY RULES IN GRAM-NEGATIVE BACTERIA***", desenvolvida no Programa de Pós-Graduação em Genética e Biologia Molecular do Instituto de Biologia da Unicamp, não versa sobre pesquisa envolvendo seres humanos, animais ou temas afetos a Biossegurança.

Assinatura: Rebeka C. V. Fanti
Nome do(a) aluno(a): Rebeka Cataldo de Oliveira Fanti

Assinatura: Rafael Miguez
Nome do(a) orientador(a): Dr. Rafael Lemos Miguez counago

Data: 04/08/2021

8.2 Declaração de direitos autorais

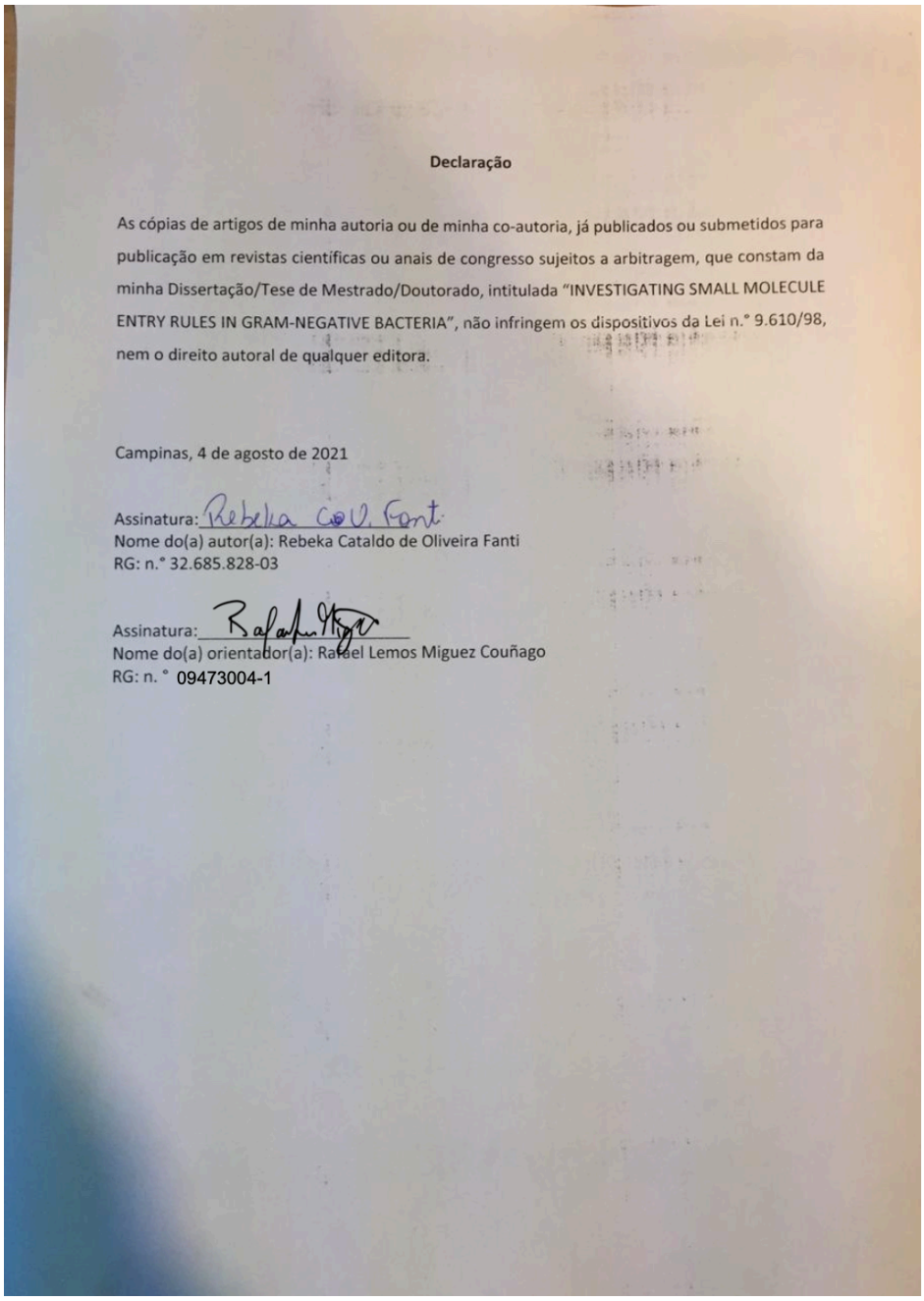

Declaração

As cópias de artigos de minha autoria ou de minha co-autoria, já publicados ou submetidos para publicação em revistas científicas ou anais de congresso sujeitos a arbitragem, que constam da minha Dissertação/Tese de Mestrado/Doutorado, intitulada "INVESTIGATING SMALL MOLECULE ENTRY RULES IN GRAM-NEGATIVE BACTERIA", não infringem os dispositivos da Lei n.° 9.610/98, nem o direito autoral de qualquer editora.

Campinas, 4 de agosto de 2021

Assinatura: Rebeka C. de V. Fanti
Nome do(a) autor(a): Rebeka Cataldo de Oliveira Fanti
RG: n.° 32.685.828-03

Assinatura: Rafael Miguez
Nome do(a) orientador(a): Rafael Lemos Miguez Couñago
RG: n. ° 09473004-1